مجلة العلوم الشاملة

Journal of Total Science

Higher Institute of Science & Technology

Raqdalen, Libya

البحوث المنشورة باللغات الأجنبية

Research Papers in Foreign Languages

Volume (6), supplement Issue (23), (Mar. 2023)

Contents

Research Papers Published in Foreign Languages

Journal of Total Science
Volume (6), Issue (23) March. 2023)
ISSN: 2518-5799

مجلة العلوم الشاملة
المجلد (6)، العدد (23)، (مارس2023)
ردمد: 2518-5799

Wavelet Transform and Entropy

Layla Wantgle Shrif Amosh

(Department of Computer Science, University of Sebha / Faculty of Education-Ghat)

نظام لتسجيل حضور الطلاب من خلال تقنية التعرف علي الوجوه باستخدام

الملخص :

أصبح تسجيل الحضور جزءًا مهما من حياتنا اليومية. يتم استخدام عدة طرق لهذه المهمة، إحداها استخدام كتاب واستدعاء الأسماء. يتم استخدام طرق جديدة ، مثل القياسات الحيوية ، لتعيين الحضور ومع ذلك ، في حين أن هذه الأساليب جديرة بالثقة وفعالة ، إلا أن لها عيوب ؛ في حالة القياسات الحيوية ، فإن أكبر عيب هو زيادة تكلفة التنفيذ. نقترح هنا استخدام طريقة التعرف على الوجوه وتجزئة الصورة والتعرف عليها لتسجيل الحضور. ان اهم ما يميز هذا العمل هو استخدامه لورقة Excel بدلاً من قاعدة البيانات. يتكون نظامنا المقترح من ثلاث مراحل:

التقاط الصورة باستخدام الكاميرا ، واكتشاف الوجوه وتجزئتها ، ثم التعرف على الوجه ، ثم تحميل اسم الطلاب الحاضرين على ورقة Excel تظهر نتائج الاختبار أن الطريقة المقترحة يمكنها تمييز الوجوه المختلفة بدقة عالية تصل إلى 98.6٪ وفي فترة زمنية قصيرة.

الكلمات المفتاحية: اكتشاف الوجوه وتجزئته –التعرف علي الوجوه– اكتشاف المميزات–خوارزمية الة المتجهات الداعمة–تقنية التحول الموجي.

Abstract

Recording attendance has become a part of our daily lives. Several ways for analyzing attendance are utilized, one of which is to use a book and call out names. New ways, such as biometrics, are being used to assign attendance; however, while these techniques are trustworthy and efficient, they have drawbacks; in the case of biometrics, the biggest negative is the increased cost of implementation. Here we are proposing the use of face detection, segmentation and recognition for recording attendance. This paper will show and test the use of face detection for marking attendance and the unique element about this model will be its use of excel sheet instead of database. Our proposed system consists of three stage: image taken

using camera, face detection and segmentation, face recognition and then load attended students name to excel sheet. The test results show that the proposed approach can distinguish different faces with a high accuracy of up to 98,6 % and in a short period of time.

Keywords Face Detection and Segmentation – Face Recognition – Feature extraction – Support vector machine– Entropy feature – wavelet transform.

1. INTRODUCTION

The present method that institutions works is that the faculty passes an attendance sheet or makes roll calls and mark the attendance of students, which occasionally disturbs the discipline of class and this sheet further goes to the admin department, which is then updated to automation on university. This process is hectic and time–consuming.

Face recognition is technology which is used to identify a person from a video or photo source [1].face recognition technology becomes gradually mature and widely used in human daily life. It has been used increasingly for forensics by law enforcement and military professionals. So, why not shift this technology to an advance automated attendance system which functions on face recognition technique? Be it a classroom or entrance gates it will mark the attendance of the employees, professors, students etc. In this work we present face recognition system for Student attendanceusing skin color skin color for segmentation the face, then Entropy and wavelet transform areused for feature extraction and finally, Support Vector Machine are used for classification process.

2. LITERATURE REVIEW

The main reason behind this section is to present topics similar to our topic in order to identify the shortcomings of the previous proposed

systems and the difference between the previous systems and our current system. [4,5,6]

By [7] an attendance system with a new method called continual monitoring has proposed, and student attendance reported dynamically by the camera capturing the image of a student in the classroom. The design of the network is simple as the class wall is fitted with two cameras. The first is a camera that captures the image of students in the classroom; the other is a sensor camera to capture the chair of a student. The program compares the image taken from a camera that records photographs and faces in the database that made a lot of time to make the attendance great. By [8] there paper implemented in the automated attendance management system a real-time computer vision algorithm. The system installed the non-intrusive camera capable of snapping images in the classroom and comparing the captured face with faces within the system from the camera's image. The approach often uses techniques that are often used in computer vision for machine learning. Haar classifiers were used in camera capture images to train.

By [9] an integrated attendance management system was implemented using face recognition techniques. The system provides matching requests and adding new information to the database. Request Matching's first move is to open the shutter and snap the picture after removing the front face. The next step is to classify the face with the training data and to paper the extracted face onto the main feature visualization.

By [10] a smart attendance marking system that involves two differentiating algorithms such as Principal Component Analysis and

Artificial Neural Network had proposed.By [11] an advanced attendance management system had proposed in which only PCA was used.

By [12] they discussed recent developments in the topic in their paper.

By [13] they report, discussed face recognition using PCA, LDA, and LBPH.

3. METHODOLOGY

Face Recognition System for Student Attendance provides a wide foundation for Face Recognition System For Student Attendance. The system is divided into five major phases. The steps of the system can be summarized as show in figure 1:

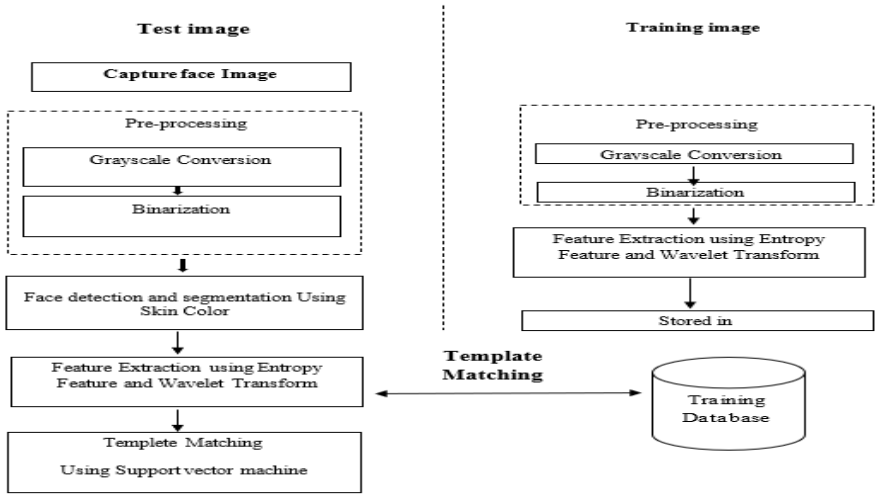

Figure 1. Overview of the proposed system

A. Capture image using camera

The camera captures a picture to persons, and the system also allows the loading of a previously saved image on the computer; figure (2) showan image for some persons loaded to our mat lab gui.

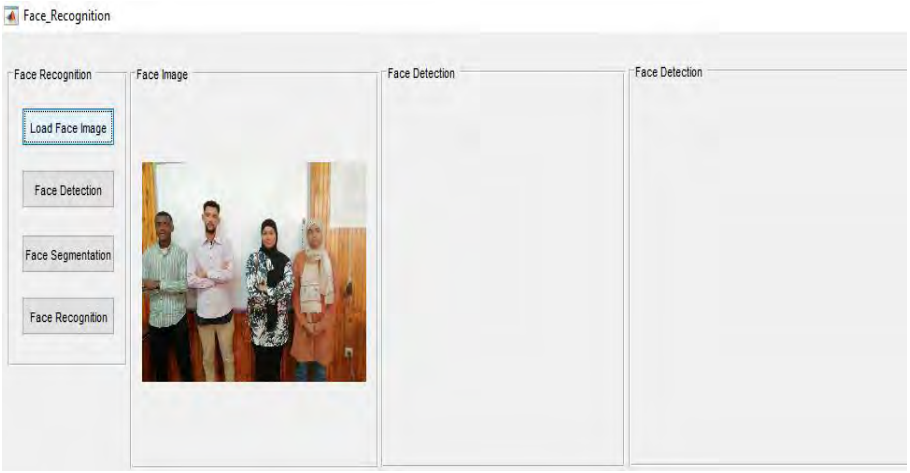

Figure 2. An image for some persons loaded to our matlab gui .

B. Face detection and segmentation Using Skin Color

Skin color method is used for detection and segmentation the face from the input image. The steps of detection and segmentation of the face can be summarized as follows [14]:

Step1: Read an image as shown in figure 1.

Step 2 : Convert the image from to one of the two color spaces listed below, and. The color space has luminance and chromatic or pure color components. This color space is distinguished from normalized RGB by the equation (1):

$$\begin{bmatrix} Y \\ Cb \\ Cr \end{bmatrix} = \begin{bmatrix} 16 \\ 128 \\ 128 \end{bmatrix} + \begin{bmatrix} 65.481 & 128.553 & 24.966 \\ -37.797 & -74.203 & (1)\ ) \\ 11200 & -93.786 & -18.214 \end{bmatrix} \begin{bmatrix} R \\ G \\ B \end{bmatrix}$$

Step3: According to the literatures [15,16,17] the segmentation of skin pixels can be performed by using the chromatic red and blue component values .

Step4: Removing the any remain small connected pixels using the morphological operator.

Step5: Filling the holes within the skin. These holes are indeed the background pixels which are not connected to the image border. They are filled easily using a dilation of the skin (bright) pixels in the image resulted from the previous step. Obviously, the dilation is authorized only on the boundaries of holes.

Step6: Face extraction. The purpose of the segmentation in the proposed system is to extract the face image.

Figure (3) showFace detection and segmentation Using Skin Color process.

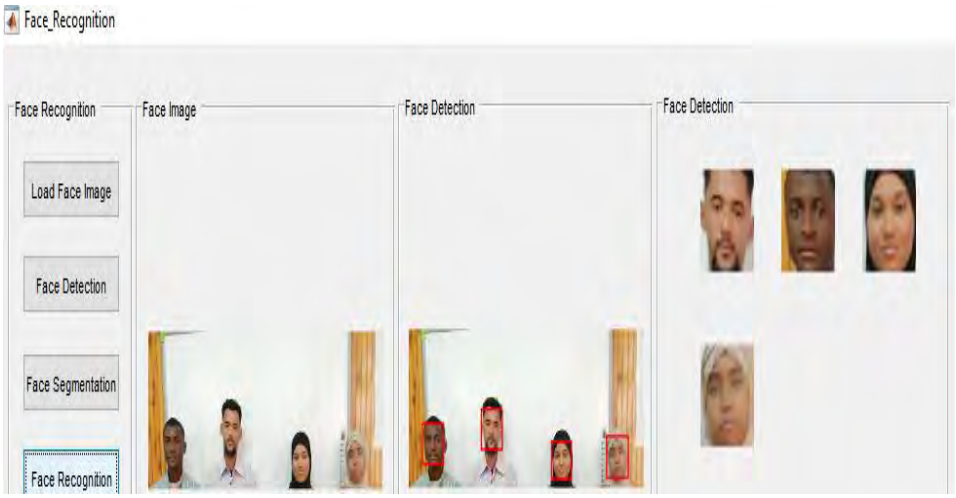

Figure 3. Face detection process

C. Feature Extraction steps

At this step, the attributes are extracted using entropy andwavelet transform as shown in the following steps:

- **Wavelet Transform:**

Two-dimensional wavelet packet decomposition. Wavelets provide an alternative to classical Fourier methods for one and multi-dimensional data analysis and synthesis, and have numerous applications both within mathematics (e.g., to partial differential operators) and in areas as diverse as physics, seismology, medical imaging, digital image processing, signal processing and computer graphics and video[18].The main advantage of wavelets is that they have a varying window size, being wide for slow frequencies and narrow for the fast ones, thus leading to an optimal time–frequency resolution in all frequency ranges [19].

Furthermore, owing to the fact that windows are adapted to the transients of each scale, wavelets lack of the requirement of stationary. Wavelet decomposition uses the fact that it is possible to resolve high frequency components within a small-time window, and only low frequencies components need large time windows. This is because a low frequency component completes a cycle in a large time interval whereas a high frequency component completes a cycle in a much shorter interval. Therefore, slow varying components can only be identified over long-time intervals but fast varying components can be identified over short time intervals. Wavelet decomposition can be regarded as a continuous time wavelet decomposition sampled at

different frequencies at every level or stage [20]. Discrete wavelet transforms (DWT) had implemented in our paper. Figure (4,5) shown Two-dimensional discrete wavelet transform and 2D wavelet packet tree for a two-level decomposed image.

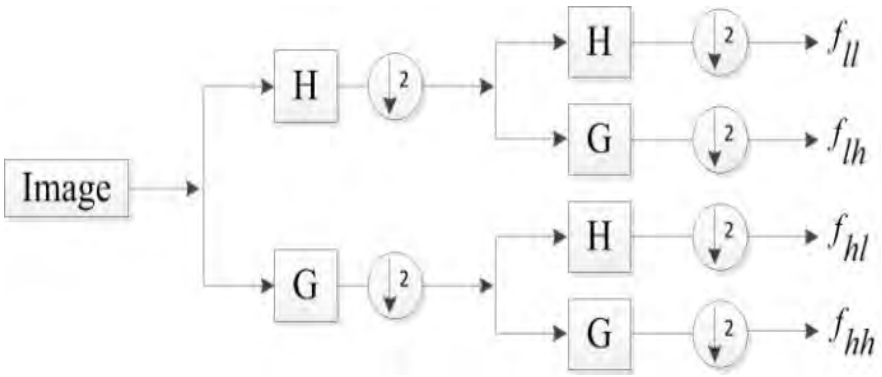

Figure 4. Two-dimensional discrete wavelet transforms

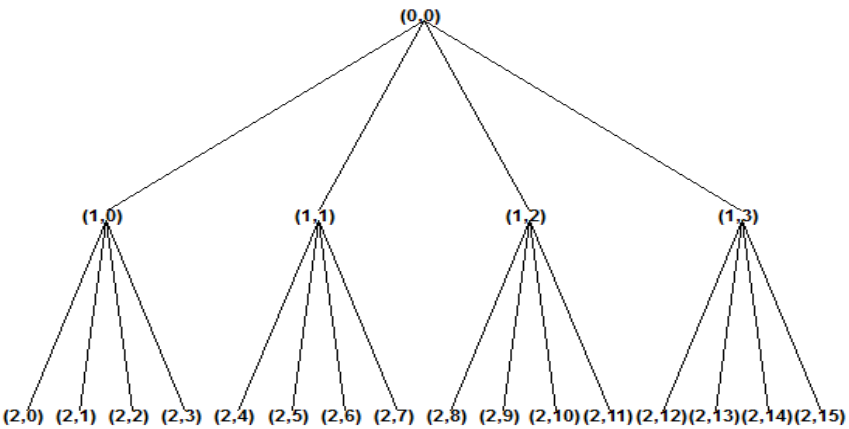

Figure 4.2D wavelet packet tree for a two-level decomposed image.

- **EntropyFeature:**

Entropy feature: An Entropy-based criterion describes information-related properties for an accurate representation of a given signal. Entropy is a common concept in many fields, mainly in image processing and signal processing. The Shannon entropy is measured as follow equation blew [21]:

$$\sigma_p^2(k) = \sum_x \sum_y [C_k^p(\quad ^{(2)} \quad]^2$$

Where $\sigma_p^2(k)$ is the energy of the texture projected to the subspace at node (p,k).

D. Classification using support vector machine

Classification using SVM consist of two steps:

- **Procedure for training**

The training of a Support Vector Machine is the process through which the Support Vector Machine learns the pattern of a face image. The training technique involves learning the patterns in the training face image and producing a Support vector classifier as a consequence. In the recognition process, the task of training data is crucial [22].

- **Procedure for classification**

Following the collection of face feature vectors, it is critical to detect the pattern of the face based on these extracted characteristics, which should be taught by a good classifier for a face recognition system [23]. Following the completion of the feature extraction procedure, the name of

the face must be determined [24]. This assignment was solved using the vector machine classifier. SVM is a newly developed machine learning technique that is already being used to identify public domain. Figure (5) Show space representing the features of the data samples using SVM.

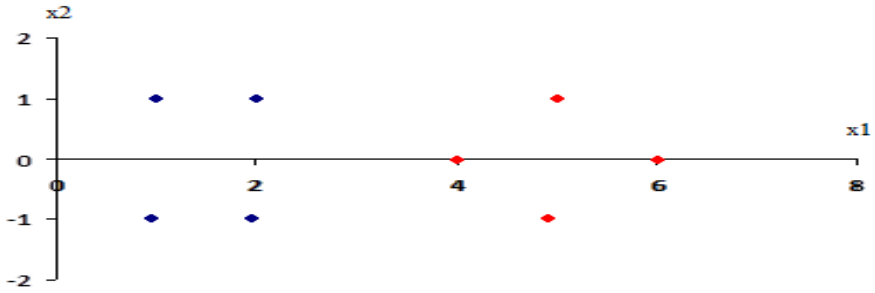

Figure 5.The space representing the features of the data samples using SVM.

4. Score attending students name to excel sheet.

After the previous operations and based on their results, after the face identification process, the name of each face of person or student is identified. The results are recorded in a new excel file created by our system, and the results are also displayed in our matlab gui as shown in figure (6).

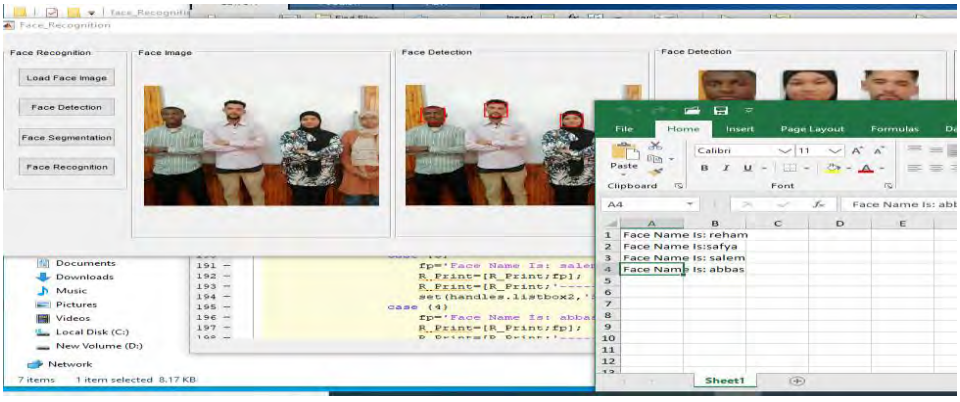

Figure 6. Student name display in created excel sheet

5. IMPLEMENTATION

Matlab is used to the execution of our system. All photos in our collection are taken by camera, and all images have pre-processed by segmentation, detection and normalization then support vector machine has used to classification process.

6. Splitting a dataset

Our dataset was divided into two distinct data sets, with 80 % and 20 % utilized for training and testing, respectively.

7. Experimental Results

This work is divided into five stages:

Step 1: Generate Training Data as the system taken images, is first trained and stored to the database. When is discovered and identified This information will also be used to compare the recognized photos in all of the uploaded files and to Make a note of attendance?

Step 2: Detection and segmentation of faces Using the Skin Color option

Step 3: Using entropy and the wavelet transform, features are retrieved.

Step 4: Face Recognition and Classification: The detected photos are compared to the trained images in the database. This now identifies the images that have been detected.

Step 5: Recording attendance: The pupils who have been identified are recorded. Following the identification procedure, the database was searched for and Their attendance is recorded in an excel spreadsheet.

Using our dataset, we created and evaluated our suggested technique. As a consequence of the suggested method, we discover that the photos vary depending on the quality and characteristics of the camera employed. Based on our findings and the recommended technique, the average accuracy arrives to 98.6%. Compared to previous studies, our system has a high rate of recognition compared to previous studies.The results were evaluated from equation (3) using recognition rate [25].

$$(3)\ \text{Recognition rate} = \frac{\text{the number of success identification}}{\text{Total number of identification trials}}$$

As, the number of accurate answers is used to determine success and the number of incorrect outcomes in a trial is known as trial identification.Figure 7. Recognition rate comparisons for the three feature extraction methods.

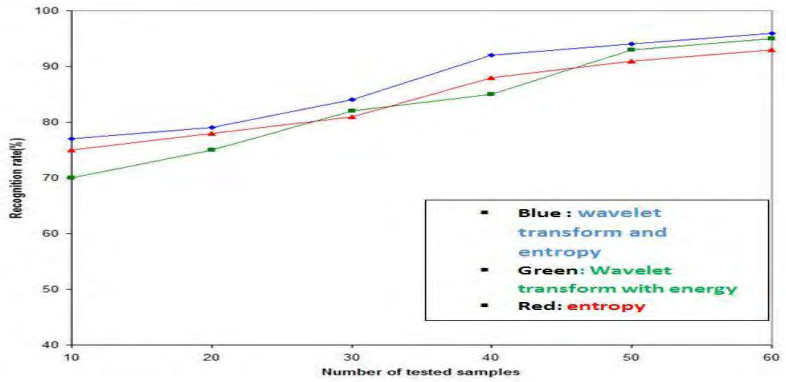

Figure 7. Recognition rate comparisons for the three feature extraction methods

8. Conclusion and Future Work

For the currently method the face recognition programmer saves time, minimizes administrative labour, and eliminates old electronic equipment. Because it simply requires a computer and a camera, the gadget does not need to be mounted by specialist equipment. Spoofing is the most serious threat to the system. As a result, a feature that shows all unrecognized faces and allows the user to manually check them may be introduced. To popularize mistakes, an automatic attendance system was designed. The effective and dependable attendance system that may replace the traditional manual procedures in the workplace environment. This approach is stable, accurate, and ready for usage. There is no requirement for specialist office equipment to attach the gadget. It is possible to design it with a camera and computer.

REFERENCES

1. Olivares-Mercado, J.; Hotta, K.; Takahashi, H.; Nakano-Miyatake, M.; Toscano-Medina, K.; Perez-Meana, H. Improving theeigenphase method for face recognition. IEICE Electron. Express 2009, 6, 1112–1117. [CrossRef]

2. Benitez-Garcia, G.; Olivares-Mercado, J.; Sanchez-Perez, G.; Nakano-Miyatake, M.; Perez-Meana, H. A sub-block-based eigenphases algorithm with optimum sub-block size. Knowl.-Based Syst. 2013, 37, 415–426. [CrossRef]

3. Hatem, H.; Beiji, Z.; Majeed, R. A Survey of Feature Base Methods for Human Face Detection. Int. J. Control Autom. 2015, 8, 61–78.[CrossRef].

4. Wang, M.; Deng, W. Deep face recognition: A survey. Neurocomputing 2021, 429, 215–244. [CrossRef]

5. McCulloch, W.S.; Pitts, W. A logical calculus of the ideas immanent in nervous activity. Bull. Math. Biophys. 1943, 5, 115–133.[CrossRef]

6. Krizhevsky, A.; Sutskever, I.; Hinton, G.E. ImageNet Classification with Deep Convolutional Neural Networks. In Advances in Neural Information Processing Systems 25; Pereira, F., Burges, C.J.C., Bottou, L., Weinberger, K.Q., Eds.; Curran Associates, Inc.: New York, NY, USA, 2012; pp. 1097–1105.

7. Redmon, J.; Divvala, S.; Girshick, R.; Farhadi, A. You Only Look Once: Unified, Real-Time Object Detection. In Proceedings of the IEEE Conference on Computer Vision and Pattern Recognition (CVPR), Las Vegas, NV, USA, 27–30 June 2016. [CrossRef] J. Imaging 2021, 7, 161 19 of 21.

8. Liu, W.; Anguelov, D.; Erhan, D.; Szegedy, C.; Reed, S.; Fu, C.Y.; Berg, A.C. SSD: Single Shot MultiBox Detector. In Computer Vision—ECCV; Springer: Berlin/Heidelberg, Germany, 2016; pp. 21–37. [CrossRef].

9. Redmon, J.; Farhadi, A. YOLOv3: An Incremental Improvement. arXiv 2018, arXiv:804.02767v1. Lin, T.Y.; Dollar, P.; Girshick, R.; He, K.; Hariharan, B.; Belongie, S. Feature Pyramid Networks for Object Detection. In Proceedings of the IEEE Conference on Computer Vision and Pattern Recognition (CVPR), Honolulu, HI, USA, 21–26 July 2017. [CrossRef].

10. Alalshekmubarak, A.; Smith, L.S. A novel approach combining

recurrent neural network and support vector machines for time series classification. In Proceedings of the 9th International Conference on Innovations in Information Technology (IIT), Al Ain, United Arab Emirates, 17–19 March 2013. [CrossRef]

11. Tang, Y. Deep Learning using Linear Support Vector Machines. arXiv 2015, arXiv:1306.0239v4. Guo, S.; Chen, S.; Li, Y. Face recognition based on convolutional neural network and support vector machine. In Proceedings of the IEEE International Conference on Information and Automation (ICIA), Ningbo, China, 1–3 August 2016. [CrossRef].
12. 14. Agarap, A.F.M. A Neural Network Architecture Combining Gated Recurrent Unit (GRU) and Support Vector Machine (SVM) for Intrusion Detection in Network Traffic Data. In Proceedings of the 10th International Conference on Machine Learning and Computing—ICMLC, Macau, China, 26–28 February 2018. [CrossRef].
13. Agarap, A.F. An Architecture Combining Convolutional Neural Network (CNN) and Support Vector Machine (SVM) for ImageClassification. arXiv 2019, arXiv:1712.03541v2.
14. Viola, P.; Jones, M.J. Robust Real-Time Face Detection. Int. J. Compute. Vis. 2004, 57, 137–154. [CrossRef].
15. Dalal, N.; Triggs, B. Histograms of Oriented Gradients for Human Detection. In Proceedings of the IEEE Computer Society Conference on Computer Vision and Pattern Recognition, San Diego, CA, USA, 20–25 June 2005. [CrossRef].
16. Ahonen, T.; Hadid, A.; Pietikainen, M. Face Description with Local Binary Patterns: Application to Face Recognition. IEEE Trans. Pattern

Anal. Mach. Intell. 2006, 28, 2037–2041. [CrossRef].

17. Dabhi, M.K.; Pancholi, B.K. Face Detection System Based on Viola—Jones Algorithm. Int. J. Sci. Res. 2016, 5, 62–64. [CrossRef].

18. Adouani, A.; Henia, W.M.B.; Lachiri, Z. Comparison of Haar-like, HOG and LBP approaches for face detection in video sequences. In Proceedings of the 16th International Multi-Conference on Systems, Signals & Devices (SSD), Istanbul, Turkey, 21–24 March 2019. [CrossRef].

19. Déniz, O.; Bueno, G.; Salido, J.; la Torre, F.D. Face recognition using Histograms of Oriented Gradients. Pattern Recognit. Lett. 2011, 32, 1598–1603. [CrossRef]

20. Antipov, G.; Berrani, S.A.; Ruchaud, N.; Dugelay, J.L. Learned vs. Hand-Crafted Features for Pedestrian Gender Recognition. In Proceedings of the 23rd ACM international conference on Multimedia—MM, Brisbane, Australia, 26–30 October 2015. [CrossRef]

21. Deng, J.; Guo, J.; Ververas, E.; Kotsia, I.; Zafeiriou, S. RetinaFace: Single-Shot Multi-Level Face Localisation in the Wild. In Proceedings of the IEEE/CVF Conference on Computer Vision and Pattern Recognition (CVPR), Seattle, WA, USA, 13–19 June 2020; pp. 5202–5211.

22. Zhang, K.; Zhang, Z.; Li, Z.; Qiao, Y. Joint Face Detection and Alignment Using Multitask Cascaded Convolutional Networks. IEEE Signal Process. Lett. 2016, 23, 1499–1503. [CrossRef]

23. Jiang, H.; Learned-Miller, E. Face Detection with the Faster R-CNN. In Proceedings of the 12th IEEE International Conference on Automatic Face & Gesture Recognition, Washington, DC, USA, 30 May–3 June 2017. [CrossRef].

24. Girshick, R.; Donahue, J.; Darrell, T.; Malik, J. Rich Feature Hierarchies for Accurate Object Detection and Semantic Segmentation. In Proceedings of the IEEE Conference on Computer Vision and Pattern Recognition, Columbus, OH, USA, 23–28 June 2014. [CrossRef].

25. Girshick, R. Fast R-CNN. In Proceedings of the IEEE International Conference on Computer Vision (ICCV), Santiago, Chile, 7–13.December 2015. [CrossRef].

Journal of Total Science
Volume (6), Issue (23) March. 2023)
ISSN: 2518-5799

مجلة العلوم الشاملة
المجلد (6)، العدد (23)، (مارس2023)
ردمد: 2518-5799

Assessment of Students Common Speaking Errors at Engineering Natural Resources College of Ajilate

AFAF HUSSIN AL HAJAJY

الملخص :

غالبًا ما تكون مهارة التحدث هي أصعب المهارات اللغوية للتعلم في الشروط. قد يستغرق الأمر سنوات عديدة من الدراسة المكثفة والتدريب قبل أن يتمكن المرء من التحدث بلغة ثانية. السبب الرئيسي الذي أدى إلى ظهور هذه الدراسة هو أن العديد من الطلاب في كليةهندسه الموارد الطبيعية بالعجيلات يواجهون مشاكل في التعبير عن أنفسهم بشكل فعال في التحدث ويواجهون العديد من الصعوبات عندما يتحدثون. لا شك في أن التحدث صعب للغاية. هذا لأنه يحتوي على قواعد معينة يجب اتباعها. من الناحية النظرية ، قد لا يكون من الصعب على معظم الطلاب تعلم هذه القواعد والأعراف الخاصة بالتحدث والاستفادة منها. لكن عندما يتعلق الأمر بالممارسة، فإنهم عادة ما يفشلون في التمسك بها. على الرغم من أن الطلاب يشددون على عقولهم لجمع الأفكار والاستفادة من الكثير من الجهد الذهني لتشكيل هذه الأفكار في جمل شفهية ؛الا انهم يرتكبون الكثير من الأخطاء. يلاحظ ريفرز (1981) أنه يجب علينا أن ندرك أن التحدث بلغة بشكل شامل هو أكثر صعوبة خاصة إذا كانت لها خصائص معينة يبدو أنها تجعلها أكثر صعوبة من المهارات الأخرى. وبالتالي يجب على المتعلم إتقان آليات التحدث باللغة الإنجليزية لتكون لغة حية.

Abstract

Speaking is the most difficult language skills in the process of learning. It may take many years of intensive study and training before one is able to speak a second language. The main reason that has given rise to this study is that many students at the natural resources college of Ajelate have problems in expressing themselves effectively in speaking and they face many difficulties when they speak.No doubt that speaking is extremely trying. This is because it has certain rules that need to be followed. In theory, it may not be difficult for most students to learn and take hold of these rules and conventions of speaking. But, when it comes to practice, they usually fail to hold fast to them.Notwithstanding that students stress their minds to gather ideas and make use of much mental effort to shape these ideas into oral sentences; they commit a lot of errors.Rivers (1981) notes that speaking a language comprehensively is much more difficult especially, if it has certain complex characteristics which make it more difficult than other skills. Thus a learner has to master the mechanism of speaking English to be a vivid language.

Keywords: Speaking skills, testing. Speaking assessment, practice, proficiency, communication

1. Introduction

Testing oral proficiency has become one of the most important issues in language testing since the role of speaking ability has become more central in language teaching with the advent of communicative language teaching.Assessment can be used to improve instruction and help students take control of their own learning. That is likely to be accomplished when assessment is authentic and tied to the instructional goals of the program. However, there are many difficulties involved in the construction and administration of any speaking assessment. Although many English teachers in natural resources college of Ajilate are interested in, communicative assessment has received little attention. If it is important to know if a person can speak a second language, then it should be important to test that person's speaking ability directly.Despite the interdependence of communicative teaching and communicative assessment (Bachman, 1990),speaking assessment in the natural resources college of Ajilate does not assess students' oral proficiency from the perspective of language use and communication. The need for classroom teachers to be equipped with some measurement tools to evaluate students' oral proficiency is becoming more and more important. Speaking assessment has become a vital part of all the examinations in every college is required, by the Ministry of Education, to perform students' speaking assessment at least once each ten days. The problem of the study is that Libyan teachers face difficulties to assess their students

speaking well. Although, they have been taught English as a curriculum subject for many years,one important difficulty facing teachers when assessing students is the communicative competence is the low English proficiency of students. Observation showed that most students at nature Resource College of Ajilate have difficulties in speaking assessment and face many difficulties when they assess speaking. The researcher discusses the Speaking Difficulties Encountered by English Language Students at Natural Resources College. The study will answer the main question: What are the difficulties and problems that face the students of English at Natural Resources College in speaking skills? &what are the suitable solutions? The following aims arise from thepresent research: identifyingthe type of difficulty encounters students in speaking, andinvestigating the suitable solutions for speakingdifficulties.

2. Speaking skill

Speaking is one of the most important language skills to be mastered by foreign students in order to interact with others for different purposes.

i.Components of speaking skill

According to Vanderkevent (1990) there are three components in speaking:

a. The Speakers are a people who produce the sound. They are useful as the tool to express opinion or feelings to the hearer. So if there are no speakers, the opinion or the feelings or the feeling won't be stated.

b. The Listeners

Listeners are people who receive or get the speaker's opinion or feeling. If there are no listeners, speakers will express their opinion by writing.

c. The Utterances

The utterances are words or sentences, which are produced by the speakers to state the opinion. If there is no utterance, both of the speakers and the listeners will use sign.

ii.The importance of speaking skills

The Importance of Speaking Skills In the present global world, communication playsa vital role in getting success in all fields. Language is used as a tool forcommunication. Perfect communication is not possible for people without using a language. Moreover, people cannot achieve their aims, objectives, and goals without using proper language to communicate. Therefore, there is a need for a language to communicate with others those who live all around the globe. As English is considered the international language and it is spoken all over the world, it serves the purpose of communicating with the people who live in different regions, states, countries, and continents of the world. Speaking skill is the most important skill to acquire foreign or second language learning. Among the four key language skills, speaking is deemed to be the most important skill in learning a foreign or second language. Brown and Yuke (1983) say, "Speaking is the skill that the students will be judged upon most in real life situations". Regardless of its importance, teaching speaking skills have been undervalued and most of the EFL/ESL teachers have been continuing their teaching of speaking skills just as memorization of

dialogues or repetition of drills. Nevertheless, the modern world demands for the requirement of communication skills for the learners and the English teachers have to teach the ELLs the needed skills so that they will improve their abilities in speaking and perform well in real-life situations. In the present EFL/ESL teaching environment, oral skills are completely neglected whereas employability depends more on communication than technology. As very less priority has been given to the important elements of language such as phonological, morphological, semantic and syntactic aspects, it has become a major impediment for the ELLs to acquire the speaking skills among the learners of English. So far, more concentration has been given to reading and writing skills. After realizing the importance of oral communication skills, more emphasis is now laid on developing the speaking skills of the learners to pursue their studies successfully and excel in their fields once they finish their education. Moreover, English is the language of getting opportunities for employment and getting success to achieve the desired goals in life.

iii. Assessing speaking skills

Assessing speaking skills is crucial part of an EFL course, assess a student's ability to speak English, and yet the difficulties in testing oral skills frequently lead teachers into using inadequate oral tests or even not testing speaking skills at all according to Chomsky1957, language teachers need to recognize the three areas of knowledge when they assessing speaking skills as the following:

1. Mechanic (pronunciation. Grammar and vocabulary)Using the appropriate words with the exact pronunciation.

2. Functions conveying the needed message from the interaction.

3. Pragmatic, social and cultural norms and rules. Understanding how to take into account who is speaking to whom, in what circumstances and for what reasons.

iv.Developing speaking skills

According to Rao(2012),the experts believe about developing skills that :

-the four skills, listening and speaking are taught and learnt in quick succession. The teacher introduces the language item in the class and learners situationalizeit.

-speech is the best introduction to other language learning skills learning through speaking is a natural way of learning a foreignlanguage.

-speech is important because it provides the opportunity for the practical usage of a foreign language.

-speech brings fluency, correction then accuracy among EFl learners; and

-It enables the teacher to use the class time economically.

3.Methodology

this part discusses the research methodologyy and steps in carrying out thisresearch proposal. The purpose of educational research according to Arthur et al., 2012 isto "*understand, inform and improve practice*". According to Creswell (2012) it is a *"process in which you engage in a small set of logical steps"* stressing that it is used to *"collect and analyses information to increase our understanding of a topic or issue"*Hegoes on to say that there are three steps that make up effective research which are, posingquestions, collecting data to answer questions and finally providing a

response to thequestion posed (Creswell, 2012).Another definition put forward by Kumar (2014) defines research as being "*The path to finding answers to your research questions constitutes research methodology*". Research methodology incorporates a range of processes to identify and elicit data for "inferences and interpretation, for explanation and prediction" (Cohen et al., 2000).

3.1. ResearchDesign

Research design is influenced by research methodologies, whether quantitative, qualitative or a mixture of both (Creswell, 2008). Making the right choices is based on identification of the issue, sample selection, accessibility and design of specifications. The whole process of embarking on research is influenced by the topic and relevant investigation rather than on chance (Cohen et al., 2007; Bryman, 2008; Henn et al., 2006).Gall et al. (2007) maintained that *"educational researchers can seldom investigate theentire population of individuals, or other phenomena, that interest them. Instead, they mustselect a sample to study*". Only once the research objectives have been set, can the target population be identified and selected (Gall et al., 2007). Initially, quantitative methods will be adopted by collating and analyzing the results of completed questionnaires collected from teachers in Natural Recourses College this will be followed by qualitative methods that will consist interviews with more open questions, to acquire a deeper understanding to support results from the quantitative data.

3.2 QuestionnaireForm (research instrument)

The researcher used questionnaires to collect the needed data from study undergraduate students at the faculty of engineering natural resources. According to Dornyeu 2007,p.102)"Questionnaire is any written instrument that present respondents with a series of questions or statements to which they are react either by writing out their answers or selecting from among the exciting answers" This study adopted a questionnaire with liker scale was used in which respondents specified their level of agreement to statements in five points. in addition, (Bell and Waters 2014,p.35 point out that this scale was used to "enhance the questionnaire responses to be clear for respondents" from the ethnical consideration side, the study participants were fully informed about the purpose of the questionnaire and the study as well.In addition, the researcher told them that the obtained data will be confidential and will only use for academic purposes.

3.3. Background of Interview Informants

After analysis of the questionnaire responses, four participants were chosen for interviews on the basis of maximum variation in age, gender, teaching experience, teaching setting, and grades taught. These four were invited to be interviewed so that their perceptions of speaking assessment could be further explored. Before the interviews with the four participants, a pilot interview was conducted with an English teaching colleague to ensure that the questions were motivating,and precise. The four individual interviews helped to collect more private interpretations of the participants' experience and opinions. Such interviews may have the characteristic of "understanding the complex behavior of people without imposing any a

priori categorization which might limit the field of inquiry". The interviews were semi-structured and conducted in a systematic order, but sometimes digressed from the prepared and standardized questions. All the interviews were conducted in Libyan so that both the interviewer and participants might understand more easily. Each interview lasted ten to fifteen minutes and was audio-taped and transcribed verbatim. The interview questions were translated into English afterwards.

4. Data Analysis and Results

Data analysis is not a simple description of the data collected analysis organization of information and data reduction. Thus, the research is required to reorganize and select related information from disordered, unorganized and discursive data. After all, analysis in qualitative research is a process of successive approximation toward an accurate description and interpretation of the phenomena; the themes and coding categories in this study emerged from a thorough examination of the data. As a consequence, recurrent themes and salient comments were identified based on the ideas provided by the participants and interview informants. In this process content analysis was performed by first listing the range of responses by the participants, and then grouping common features and recurrent themes. These themes were then subsumed under three main categories.From the responses of the participants to the questionnaire, it was found that all the participants were conducting speaking assessments at least once a year in their classrooms. However, they expressed frustration at the speaking assessment tasks in use and at the ways they conducted assessments of students' communicative competence in their classrooms. Almost all were using speaking assessment tasks which did

not reflect authentic interaction between themselves and their students. They also reported that they were not ready enough to construct and administer communicative speaking assessment.

Analysis of data revealed three main categories:

(1) Types of speaking assessment tasks used by English teachers.

(2) The teachers' perceptions of speaking assessment

(3) The practical constraints on the teachers in conducting speaking assessment to assess students' communicative competence.

4.1. Types of speaking assessment tasks used by English teachers

These responses will be discussed in detail in the following section:

- Speaking assessment tasks used by teachers
- Let the students pick up one or two questions
- Show and tell
- Self-introduction or family introduction
- Role play
- Rote memory of text dialog
- Picture description
- Information gap activity

4.2. Teachers' perceptions of speaking assessment:

The ways of speaking assessment in the classrooms assessment can be used to improve instruction and help students take control of their own learning. That is more likely to be accomplished when assessment is

authentic and tied to the instructional goals of the program. However, in this study it seemed that the speaking assessment conducted by English teachers did not reflect authentic interaction between the teacher and the students.

Firstly, teachers did not elicit students' responses as an interviewer. As a result, there was no face-to- face communication between the teacher and the students.

Secondly, teachers announced questions and tasks in advance, even though, communication is unpredictable in both form and message.

Thirdly, students' responses were not impromptu but rehearsed because of the predictable nature of tasks.

The types of non-authentic speaking assessment tasks several types of such **non**-authenticspeaking assessment tasks used by teachers were identified through this study:

Firstly, teachers used speaking assessment tasks which gave the students less. Psychological burden. As beginners in English, many Students School had a very small vocabulary and a limited number of English structures. Thus, they found assessment of their speaking by the teacher to be very stressful.

Secondly, teachers tried to lower students' affective filter (Krashen and Terrell, 1983) by minimizing the effects of unpredictable factors and anxiety. "Performers with optimal attitudes have a lower affective filter" (Krashen and Terrell, 1983:38). It will encourage students to interact with teachers with confidence. Students felt intimidated by unfamiliarity with the

test type. And also lack of preparation for the test seemed to lead them not to reflect in their performance the best that they are capable of.

Thirdly, teachers used time-saving speaking assessment tasks designed for the convenience of construction and administration because they taught large classes for relatively short periods of time and were already overloaded with excessive work in their school. They felt burdened by speaking assessment.

Lastly, teachers used the speaking assessment tasks which did not demand them to take the role of an interviewer. Such assessment tasks helped teachers function as a rater only, scoring students' responses on the basis of their promptness and the degree of preparation.

This study also indicated that teachers were not equipped with an adequate theory of communicative speaking assessment. As a consequence, the teachers had little confidence in conducting speaking assessment. Nor had the 'backwash effect' of assessment on teaching been perceived by the teachers in designing speaking assessment.

As Bachman (1990) highlighted, positive 'backwash' will result when the assessment procedures reflect the skills and abilities that are taught in the course. However, speaking assessment appeared not to be tied to the instructional goals in content. As a result, it was a 'one-off' as one-time test only. Inter-rater reliability makes an important contribution to test reliability. According to Bachman (1990), rating should be concerned with enhancing the agreement between raters by establishing explicit guidelines for the conduct of rating. However, teachers were scoring alone. They did not concern themselves with inter-rater reliability. Though they held

teachers' conference regarding speaking assessment, inter-rater reliability was not an important issue for them.

Teachers' perceptions of the practical constraints in conducting communicative speaking assessment .In addition, this study revealed the practical constraints in conducting authentic speaking assessment in the contexts of the classroom and educational system. Most of the teachers in the study appeared frustrated by the big gap between theory and practice. Participants mentioned constraints in conducting communicative speaking assessment, such as large classes and time-consuming, excessive work in addition to classroom teaching, lack of training in conducting speaking assessment, lack of effective and efficient assessment instruments, difficulty in eliciting students' responses. Consequently, most of the teachers simply did not venture to try communicative speaking assessment while others gave it up after a brief try.

Teacher's personal belief However, another factor was shown to be important in determining the use of communicative assessment, that of the teacher's personal belief in trying new ways of communicative speaking assessment, and willingness to persist, despite the practical constraints of classrooms. One teacher, when responding to the questionnaire indicated that she used picture description to elicit students' responses and endured the students' hesitation in making their appropriate responses.

5.Discussion

This study showed that teachers agreed with the necessity of speaking assessment because it motivated students. Most teachers expressed a strong desire to learn how speaking assessment can be effectively and

efficiently administered in the classroom context. Thus, teachers need to have assistance and encouragement in trying new ways of communicative assessment. Continuing support for teachers who may need help with communicative assessment is important. This can be achieved by conducting in-service teacher education programs, in which teachers have opportunities to retrain and refresh themselves in communicative speaking assessment. More importantly, teachers need to receive assistance in changing their educational theories and attitudes. This study also brought out another factor that may be specific to English teachers; teachers were overloaded with excessive work in addition to classroom teaching. It was revealed that teachers were frustrated and infuriated by this reality. If this situation is to be relieved, educational administrators need to show greater sensitivity to the teachers' complaints of excessive workload and to reflect teachers' point of view in their decision- making. One of the major reasons which teachers need to be aware of the shift in social and educational needs. All the teachers in are now required, by the Ministry of Education, to conduct speaking assessment in their English language classes. Therefore, teachers need to make conscious and persistent efforts to introduce more communicative speaking assessment into their classrooms and to be equipped with some measurement tools to evaluate their students' oral proficiency.

6. Conclusions

The present study arrives at the following conclusions:

i. To identify the types and the ways of speaking assessment used by teachers of English.

ii. Teachers' perception of the practical constraints in Classrooms, affect teachers' assessment of speaking. In terms of question 1 the study found that teacher of English did not assess students' oral proficiency from the perspective of language use and communication. This fact was reflected in the types of speaking assessment tasks used by the English teachers and in the ways they conducted speaking assessment.Several types of such non-authentic speaking assessment tasks used by the teachers were identified through this study.Teachers used speaking assessment tasks which gave the students less psychological burden.Teachers tried to lower students' affective filter by announcing tasks in advance to minimize the effects of unpredictable factors.

Teachers used time-saving speaking assessment tasks designed for the convenience of construction and administration.Teachers used the speaking assessment tasks which did not demand the teacher to take the role of an interviewer.In conducting speaking assessment, teachers were not equipped with an adequate theory of speaking assessment. For example, they seemed not to be aware of 'backwash effect' of testing on teaching, of inter-rater reliability and of the necessity to be trained in the application of assessment criteria through rigorous standardization procedures. As a consequence, teachers had little confidence in conducting speaking assessment.

iii. This study revealed the practical constraints in conducting communicative speaking assessment in the classroom context and the educational system. Participants reported such constraints as:

-Large classes

-Excessive work in addition to face- to- face classroom teaching

- Lack of training in conducting speaking assessment

-Lack of effective and efficient instruments

-Difficulty in eliciting students' responses

The findings of this study suggest that educational administrators need to show greater sensitivity to the teachers' complaints of excessive workload and to reflect teachers' points of view in their decision- making. Also, teachers need to have assistance and encouragement to try new ways of communicative assessment in their classrooms.

References:

1.Arthur. J, Waring. M. Coe. R and Hedges.L. (2012) Research Metods& Methodologies in Education. Los Angeles. USA: SAGE Publications Ltd.

2.Bachman, L.F. (1990): Fundamental Considerations in Language Testing. Oxford: Oxford University Press.

3.Bryman. A. (2008) Social research methods. 3rd ed. Oxford: Oxford University Press

4.Bell, J and Waters,S.2014(p.35)Doing your research project a guide for first time research 6thedn.Maidenhead,Berkshire:Open University Press.

5.Brown, G.,Yule, G . (1983). Discourse Analysis .New York : Cambridge University Press.

6.Creswell. J. (2008) Educational research: planning, conducting, and evaluatingquantitative and qualitative research. 3rd ed. New Jersey: Pearson Merrill Prentice Hall.

7.Creswell. J. (2012) Educational Research: Planning, Conducting and Evaluating Quantitative and Qualitative Research (4th ed.). Boston: Pearson

8.Cohen. L. Manion. L. and Morrison.K. (2007) Research methods in education. 6th ed. London: Routledge

9.Chomsky,N. (1957) . Syntactic structure .The Hague:Mouton .

10.Dornyei,z.(2007)research methods in applied linguistics.Oxford;Oxford university press.

11.Gall. M, Gall. J and Borg. W. (2007) Educational Research: An Introduction 8th (ed). Boston: Pearson.

12.Henn. M, Weinstein. M and Foard.N (2006) A Short Introduction to Social Research. London, New Delhi: Sage Publications.

13.Kumar. R. (2014) Research Methodology.(4th edn).London. Sage.

Cohen, L. Manion. L. and Morrison.K. (2000) Research methods in education. 5th ed. London: Routledge.

14.Krashen. S and Terrell. T. (1983) The Natural Approach: Language Acquisition in the Clasroom: Alemany Hall Europe. London

15.Krashen, S.D & Terrell, T.D. (2000, second impression): The Natural Approach, Language Acquisition in the classroom. Longman, Pearson Education Limited, England.

16.Rao,V K.2012.Techniques of Teaching English .Hyderabad:Neelkamal Publications.

17.Rivers , Wilga M .(1981)Teaching Foreign Language Skills: University of Chicago Press.

18.Vanderkevent,1990.Teaching speaking and components of speaking .New York: Cambridge University Press.

Appendix

QUESTIONNAIRFORM

Name:----------

Age:----------

Grade:----------

Educational Level:----------

Experience:----------

1. When you are choosing speaking tasks; do you involve the students in the choice of topics? If so, how do you decide?
2. How do you evaluate the speaking tasks you are doing?
3. Many students have problems getting started to write. How do you

Work on that issue?

4. Do you have any particular methods to create a specific

Atmosphere for speaking sessions?

5. What do you think is an appropriate group size for discussions?
6. Do you speak only English in class?
7. How do you manage to get the students to speak only English?
8. Role play is said to be a good way of improving students'

Speaking abilities. Do you ever use this method?

9. How do you evaluate whether a students' speaking skills have

Developed or not?

10. How do you make sure that everybody gets to speak as much as Possible?

Journal of Total Science
Volume (6), Issue (23) March. 2023)
ISSN: 2518-5799

مجلة العلوم الشاملة
المجلد (6)، العدد (23)، (مارس2023)
ردمد: 2518-5799

Detection of radon gas in some building materials stores in Surman, West Libya

Aliya M Kishada

University of Zawia – Zuwara Faculty of Education – Physics Department

Abstract:

The aim of this study was to detect the existence of the radioactive radon gas in ceramic building materials companies. A total of twelve ceramic stores in these companies were used in this study. The measurements were carried out using the sensitive Solid State Sensor, which is known as (RADEX MR107), The highest activity value of radon gas in some of these stores was found to be (80 Bq/m^3) while the lowest value was found to be (30 Bq/m^3). In addition, the average activity ranges from 22 Bq/m^3 to 39 Bq/m^3 Most of the results obtained are lower than the world standard limits given by ICRP [1]. These results show that the radioactive radon gas exists in these stores within the safety limits. The total effective doses per annum due to ingestion and inhalation of radon occurred in the ceramic stores were found to range from 0.24 mSv/y to 0.43 mSv/y which are also within the safety limits.

Keywords: building materials, natural radioactivity, granite, radon, exhalation.

1-Introduction:

It is well known that human beings are continuously exposed to ionizing radiation in their homes and work places. Every building material used in these places such as sand, soil, cement, ceramic, marble and rock or any

other building materials contain a natural share of Uranium, Thorium and Radium. The building materials derived from rocks and soil contain

these natural radio nuclides. The decay of theses radio nuclides leads to the emission of the radioactive radon gas. Its decay products are formed and released from the building materials mentioned above. Furthermore, The amount of radioactivity in building materials depends on the type of material used. Radon gas is one of the most dangerous types of radiation and the closest to humans. This radioactive gas has a half-life of 3.8 days. It is the most stable isotope as it is a chemically inert gas that is colorless, tasteless and odorless. Its atomic number is 86 with a density of (9.7 kg/m^3)

and a boiling point equals to ($-61.80\ ^{o}$C) [2]. It is a radioactive noble gas emitted by the decay of ^{226}Ra, an element of the ^{238}U decay series [3]. ^{222}Rn decays into a series of other radioactive elements, of which ^{214}Po and ^{218}Po are the most significant, as they contribute the majority of radiation dose when inhaled. Through a number of decay series, ^{218}Po transforms into ^{210}Po and it decays into stable ^{206}Pb as it is shown in figure (1). The ^{222}Rn and its decay products are reported as major causes of lung cancer [4]

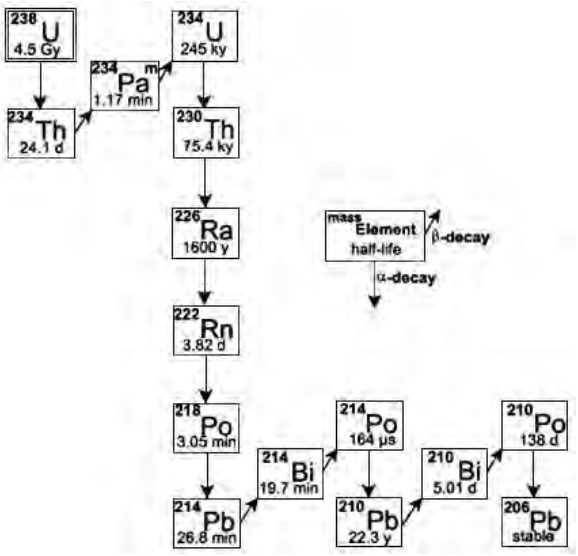

Figure (1): shows Uranium decay series. [5]

Concentration of radon gas inside building material stores is expected to be high and is a major contributor to the ionizing radiation dose received by the workers in these stores .Evaluation of health effects due to exposure to ionizing radiation from natural sources requires knowledge of its distribution in the environment. The estimated average annual dose of the population receiving natural radiation is 2.4 mSv [6]. It is well known that the inhalation of radon (^{222}Rn) and its radioactive decay products, contributes more than 50% of the total radiation dose to the world population from natural sources [7].

2-Materials.

2.1- Radon Gas Detector.

A sensitive Solid State Sensor, which is known as (RADEX MR107), was used in this research to measure the concentration of radon gas (^{222}Rn) radiating alpha (α) particles in the air of a number of ceramic stores and the measurement process using this device is subject to a number of variables, namely temperature, Moisture percentage and detection time. Figure (2) shows the(RADEX MR107) device used in this study.

Figure (2): The (RADEX MR107) device used in this research.

2.1.1-Device Description:

The (RADEX MR107) device used in this research uses a modern method of electrostatic deposition of daughter decay products on a semiconductor sensor, followed by detection of charge-sensitive preamplifier. It helps to monitor the microclimate in the room, by measuring the temperature and humidity, while keeping the results in the device's memory. In case of detection of dangerous level of radon, the device will inform about it by a sound signal. Also, Software RAD Data Center, allows the view the dynamics of radon, temperature, humidity measurements. And export the results of measurements and make individual settings of the

device. Tables (1 and 2) bellow show the specifications of the (RADEX MR107) device used in this research.

Table (1): Technical details of the Radon gas detector.[8]

Technical Details	
Manufacturer	Quarta-Rad
Part & Model Number	MR107
Device Weight	10 Ounces
Device Dimensions	6 x 2.2 x 3 inches
Power Source	AC
Display Style	LCD

Table (2): Features and capabilities of the Radon gas detector (RADEX MR107).[8]

Features and capabilities		
Measuring cycle	H	1
Battery run time in measuring mode	H	140
Maximum stored data points		1000
Detection range of EEVA radon	**Bq**/m^3	< 30 to 9999
Audio alarm thresholds of EEVA	**Bq/m^3**	< 30 to 9999
Operating temperature range	°C	+10 to +35
Data transfer method		USB

Dimensions	155 x 80 x 58 mm
Battery type	Internal Li-Ion battery
Measuring the volume activity of radon in the air (EEVA)	
Relative humidity and air temperature	
Detects dynamic changes in gas concentration	
Adjustable audio alarm that reacts to excessive EEVA levels of radon tracking of dynamic changes in radon EEVA, air temperature and relative humidity	
Calculating minimal, median and maximum values of radon EEVA, air temperature and relative humidity	
Storing gathered data in internal memory	
Transferring stored data to Windows PC for analysis	
Working with data via Windows PC software	
Sounds an alarm when the gas levels are no longer safe	

Figure (3) below shows a sample of some data and environmental factors affecting radon gas activity presented by the device during measurements.

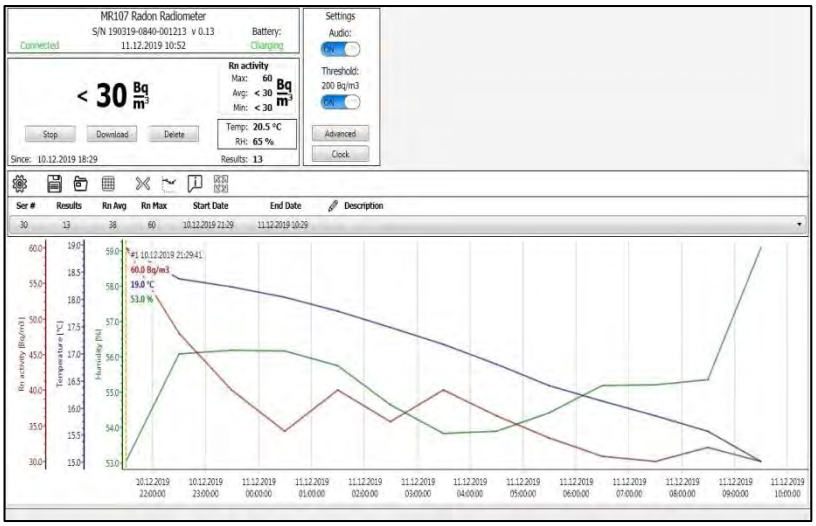

Figure : (3) A sample of some data and a spectrum of environmental factors

3-Detecting Method:

The indoor radon concentrations in this study were determined by using the sensitive Solid State Sensor (RADEX MR107). This detector makes it easy to detect the existence of the radioactive radon gas in many places such as, houses, schools, hospitals and other buildings. In this study we used this detector to detect the radon gas in building materials (ceramic) stores in Surman city which is located in the west of Tripoli, Libya as shown in figure (4) below. The device was put in twelve ceramic stores in places where it is far from ventilation and air conditioners and it was left for 24 hours to detect the existence of the radioactive radon gas. After this period it was connected to the laptop to import the data obtained from the measurements

Figure (4): Shows the area of study.

4- Results and Discussion:

Indoor radon measurements were carried out in 12 ceramic companies. Table (3) shows the experimental results of concentration of radon gas detected in these stores. The period of the measurements of the concentration of the radon gas was 24 hours for each store. During these measurements, It was found that the highest value of radon gas detected was (80 Bq/m3), this high value of radon gas concentration was due to the lack of ventilation. The lowest value detected was (30 Bq/m^3), the reason of this low value detected was due to the frequent ventilation in these stores. Effective dose due to exposure to radon and progenies were also calculated. As stated in Table (3), the highest value of the annual effective dose was found to be (0.43 mSv/y) whereas, the lowest value was found to be (0.24 mSv/y). All the calculated values of annual effective dose were below the ICRP recommended level of 1 mSv per year. Table (3) below presents the results obtained from the detection of the radioactive

radon gas in the building materials stores. Figures 5, 6 and 7 shown below present the plot of the maxim and average of the radon gas activity and the annual effective dose, respectively. The annual effective dose of exposure to indoor radon gas was calculated using the equation below [9].

$$D_R\ (\text{mSv/y}) = (\ 0.17 + 9 \times F_R\ ) \times C_R \times 8760 \times H \times 10^{-6} \qquad (1)$$

where D_R is the annual effective radiation dose of exposure to ^{222}Rn. The values of 0.17 and 9 are dose conversion factors for the concentrations of ^{222}Rn and its progeny, respectively, in nSv [10]. F_R is the equilibrium factors for ^{222}Rn and its progeny and worldwide typical F_R value is 0.4. C_R is the concentrations of ^{222}Rn in Bq/m^3, and 8760 is the number of hours in a year. H is the occupancy factor, and its values are 0.50 (12 h/24 h), 0.33 (8 h/24 h) and 0.17 (4 h/24 h) in indoor working environments. A multiplication factor of 10^{-6} is adopted to convert nSv into mSv.

No	Store code	Source	Radon Activity CRn [Bq/m^3]			Annual effective dose (mSv/y)	Temperature (°C)	Humidity (%)
			Max	Min	Avera			
1	cer110	China–Egypt	30	30	30	0.33	28	54
2	cer120	India–Egypt	60	30	33	0.36	26	53
3	cer130	China–Spain	40	30	31	0.34	28	64
4		China–	40	30	31			

	cer140	Spain				0.34	27	62
5	cer150	India–Egypt	80	30	39	0.43	36	40
6	cer160	Egypt–Turkey	34	30	22	0.24	33	48
7	cer170	Spain–Egypt–Algeria	30	30	30	0.33	32	41
8	cer180	Egypt–Tunisia	34	30	30	0.33	29	53
9	cer190	China–Egypt–India	37	30	31	0.34	32	59
10	cer200	China–Spain	40	30	31	0.34	29	43
11	cer210	India–Spain–Tunisia	48	30	33	0.36	29	55
12	cer220	China–Spain	34	30	31	0.34	27	53

Table (3): Concentration of radon gas in ceramic stores.

Figures (5 and 6) show the chart of the maximum and the average values of radon while figure (7) shows the chart of the annual effective does values of radon gas concentration obtained from this study.

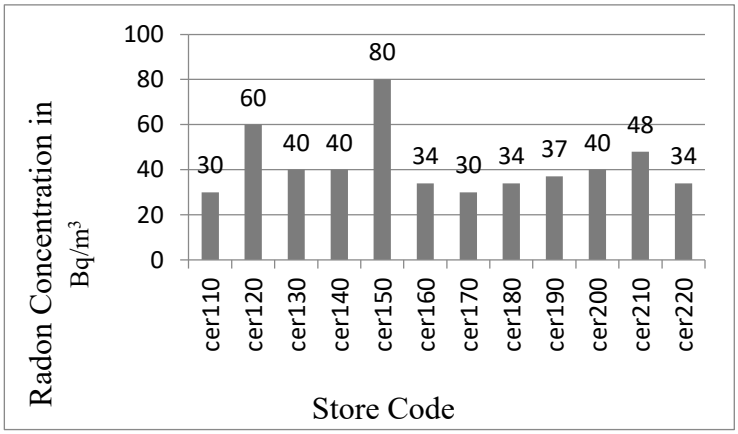

Figure (5): Shows maximum values of radon gas concentration.

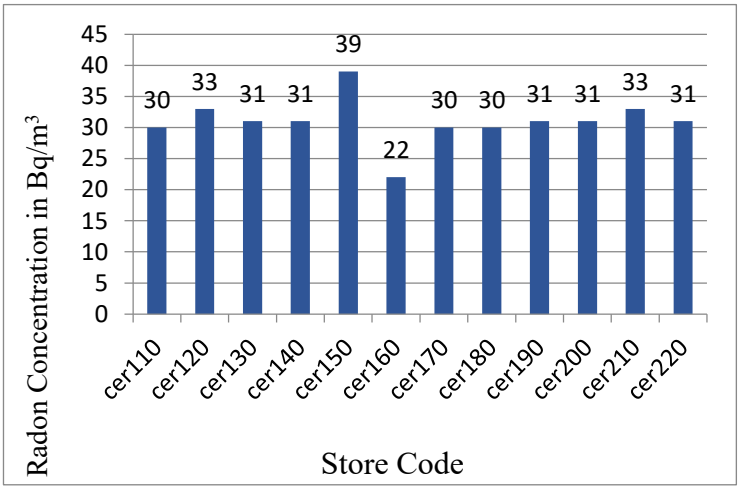

Figure (6): Shows average values of radon gas concentration.

Figure (7): Shows the annual effective does values of radon gas concentration.

5- Conclusion:

In the present study, we detected the radioactive radon gas in the indoor environment of some building materials stores (ceramic stores). The values of radon concentration found in building materials stores were well below the range prescribed by the UNSCEAR [10]. These low values of radioactive radon gas are unlikely to harm human health. The highest activity of radioactive radon gas in this study was found to be .The total effective dose per annum due to ingestion and inhalation of radon occurred in ceramic stores are ranged from 0.24 mSv/y to 0.43 mSv/y which is also within the safety limits.

6- Acknowledgements:

The author acknowledges, with gratitude, the assistance received from the owners of companies which were involved in this study.

7- References.

[1].International Commission on Radiological Protection (ICRP) (1987) Lung Cancer Risk from Indoor Exposure to Radon Daughters Oxford. ICRP Publication 50: 17.

[2]. Department of Environmental, 1995. A Guide Risk Assessment and Risk Management for Environmental Protection, HMSO, London, U.K., p.78-95.

[3] Appleton JD. Radon: sources, health risks, and Hazard mapping. AMBIO: A Journal of the Human Environment. 2007. 10.1579/0044-7447(2007)36 [85:rshrah] 2.0.co;2.

[4]. International Commission on Radiological Protection ICRP (1984) Non stochastic Effects of Irradiation. ICRP Publication.

[5] Google web sight

[6] Ismail AH, Jaafar MS (2011) Interaction of low-intensity nuclear radiation dose with the human blood: using the new technique of CR-39 NTDs for an in vitro study. Appl Radiat Isot 69: 559-566.

[7] Ismail AH, Jaafar MS (2010) Indoor radon concentration and its health risks in selected locations in Iraqi Kurdistan using CR-39 NTDs. The 4th International conference on Bio information and Biomedical Engineering (iCBBE 2010), 18-20 June, Chengdu-China.

[8] Quarta-Rad Ltd, Inc. RADEX MR107 Advanced Radon Gas Detector. User Manual, 2017.

[9] Lubin JH and Boice JD. Estimating Rn-induced lung cancer in the united states. *Health Physics*.1989;57(3):417-427.doi:10.1097/00004032-198909000-00008[PubMed][CrossRef] [Google Scholar]

[10] UNSCEAR. Annex B: Exposure from natural radiation sources. United Nations. 2000[Google Scholar]

Journal of Total Science
Volume (6), Issue (23) March. 2023
ISSN: 2518-5799

مجلة العلوم الشاملة
المجلد (6)، العدد (23)، (مارس2023)
ردمد: 2518-5799

Solar Energy Driven Seawater Reverse Osmosis (RO) Desalination Technology in Libya

Abdul hamid N. Elghemi*

University of Gharyan, Libya

الملخص :

ليبيا ، مثل العديد من البلدان الأخرى في المناطق القاحلة ، تعتمد بشكل كبير على موارد المياه الجوفية. في عام 1998 ، قدرت سعة إمداد المياه الجوفية المتاحة بحوالي 2.557 مليون متر مكعب في السنة ، وهو ما يمثل 95.6٪ من إجمالي الإمداد ، وساهمت المياه السطحية بنسبة 2.7٪. وبالمقارنة ، كانت تحلية مياه البحر وإعادة استخدام المياه العادمة موارد ثانوية بحصة صغيرة جدًا بلغت 1.4٪ و 0.7٪ على التوالي . وبالتالي ، فإن إجمالي سعة إمداد المياه يساوي 3843 مليون متر مكعب. وسجل القطاع الزراعي أعلى كمية استهلاك بنسبة 85٪. يستهلك القطاع المنزلي 11.5٪ فقط ، والقطاع الصناعي يستخدم 3.5٪ فقط ، وهو ما يمثل أقل نسبة من إجمالي المياه المسحوبة. تظهر الكميات عدم تناسب بين إجمالي المسحوب والحجم السنوي المتاح لموارد المياه المحلية. من الواضح أنه كان هناك عجز أدى إلى تدهور كمية ونوعية المياه بسبب تسرب مياه البحر، جعل استخدام تقنيات تحلية المياه المختلفة ليبيا واحدة من الدول الرائدة في هذا المجال المحدد على مدار الأربعين عامًا الماضية، أدى إهمال أهمية الموارد المائية غير التقليدية وعلاقتها بالموارد التقليدية في موازنة الوضع المائي في ليبيا إلى تأخير تطوير تقنيات تحلية المياه في العقد الماضي. ووفقًا لهذه الأرقام ، فقد انخفض المتوسط السنوي الوطني لتوافر المياه للفرد من 2280 مترًا مكعبًا في عام 1955 إلى 380 مترًا مكعبًا في عام 2005 ، ومن المتوقع أن يصل إلى 190 مترًا مكعبًا بحلول عام 2050. وبالتالي ، فإن الدولة بأكملها تعاني بالفعل من ندرة المياه التي تزداد حدة مع مرور الوقت. علاوة على ذلك ، تم تقدير إجمالي العرض المتاح من المياه العذبة على أساس ثابت بمعدل ثابت قدره 2279.5 مليون متر مكعب في السنة. بالإضافة إلى ذلك ، فإن وجود الأراضي الخصبة والأنشطة الصناعية على طول الساحل ذي المناخ المعتدل يتسبب في تركز السكان في هذه المناطق ، مما يؤدي إلى توزيع غير متساوي للسكان وعجز كبير في إمدادات المياه.

الكلماتالمفتاحية: التناضح العكسي; (RO) عملية تنقية المياه ، أيونات منفصلة ،غشائية منفذة جزئيًا.

نظام الكهروضوئية; (PV) نظام الطاقة الشمسية ، نظام الطاقة الكهربائية ، إمدادات مصممة، وسائل الطاقة الشمسية.

Abstract

Approximately 1.2 billion people worldwide do not have access to adequate clean water the reasons for which vary with location [1]. Many of the people living in the Middle East and North Africa (MENA) are experiencing a shortage of fresh water sources due to the continuous growth of the population and economy in this region, increase of urbanization and industrialization, as well as climate change. Libya which is located in North Africa on the Southern coast of the Mediterranean Sea is one country experiencing such shortages. Libya lies between 200 N and 320, 55" N latitude, and between 100 E and 250 E longitude. The area of Libya is 1,750,000 km_2, 88% of which is desert or semi desert land. The coast is 1955 km long, facing the European continent. Over 90% of the 6 million inhabitants live on a thin strip along the coastline.

Libya has serious water shortage problems due to the fact it is located in an arid and semi-arid zone known for its scant annual rainfall, very high rates of evaporation, and consequently extremely insufficient water resources. The average temperature year round is 26 ^{0}C, with the world's highest temperature in the shade of 58 ^{0}C, recorded in El Azizia (32.32^0 N and 13.35^0 E) in the desert [2]. For about a decade, the exploitation of freshwater in this region has surpassed the available renewable surface and groundwater sources. In addition, Libya does not have a permanent flow of fresh surface water resources due to the lack of rainfall fluctuation rate and the nature of the geological formations. The annual rate of rainfall in Libya ranges between 100 and 500 mm.

Keywords:Reverse osmosis (RO);water purification process, uses a partially permeable, membrane separate ions.

Photovoltaic (PV) system; **solar power system**, electric **power system,** designed supply usable, **solar power** means.

1. Introduction

Libya, like many other countries in arid regions, is heavily dependent on groundwater resources. In 1998 the available groundwater supply capacity was estimated to be 2,557 million cubic meters per year, which represents 95.6% of the total supply, and the surface water contributed 2.7%. In comparison, the desalination of seawater and the reuse of wastewater were minor resources with very small shares of 1.4% and

0.7%, respectively [3]. Thus, the total water supply capacity equals 3,843 Mm^3.

The agricultural sector had the highest consumption quantity at 85%. The domestic sector consumed only 11.5%, and the industrial sector used only 3.5%, representing the lowest portion of the total water withdrawal [4]. The quantities show a disproportion between the total withdrawal and the annual available volume of local water resources. Clearly, there was a deficit, leading to deterioration of both water quantity and quality due to seawater intrusion [5].

The use of different desalination technologies has made Libya one of the leading countries in this specific field over the past 40 years. Neglecting the importance of nonconventional water resources and its relation to conventional ones in balancing the water situation in Libya has caused a delay in developing desalination techniques in the last decade. According to these figures, the national annual average per capita water availability has been reduced from 2280 m^3 in 1955 to 380 m^3 in 2005, and is expected to reach 190 m^3 by the year 2050. Thus, the whole country is already experiencing water scarcity that is becoming increasingly severe with time.

Furthermore, the total available supply of fresh water on a consistent basis has been estimated at the fixed rate of 2279.5 million cubic meters per year.In addition, the presence of fertile land and the industrial activities along the mild climate coastline cause the population to be concentrated in these areas, resulting in an uneven population distribution and huge water supply deficits.

1.1 Water Shortage Problems in Libya

To overcome the problem of water shortage, Libya has achieved one of the largest civil engineering projects in the world known as The Man-Made River Authority (GMRA), at a cost of approximately US $27 billion. The purpose of the project was to transfer around 6.5 million m^3/d from groundwater basins in the south to the coastal areas in the north through a network of large concrete pipes with a diameter of 4 m and a length of 4000 km buried under the desert sand to eliminate evaporation.

The pipeline is supplied by more than 1,300 wells, most of them over 500 m deep. However, over-exploiting the groundwater reserves in the southern region showed poor management of the natural resources in Libya and consequently this project resulted in negative environmental and economic implications that will be discussed in later chapters.

Since lack of water is a major factor affecting the agricultural and industrial development, water desalination techniques have emerged as a solution to water shortages. The most common desalination method uses reverse osmosis membrane technique and the electric power needed for this operation is mostly generated from fossil fuels.

However, increased fuel prices and concernsover environmental pollution caused by the use of fossil fuels are triggeringa push to shift to alternative sources of energy. Solar energy can be a great solution to the environmental concerns since it is a clean source of energy and solar radiation is abundant in this region all year round. Hence, solar power could be one of the most successful applications of solar energy in most of those hot climate countries with limited resources of fresh water. Solar

averageglobal radiation on coastal and desert areas in Libya as shown in Figure 1.

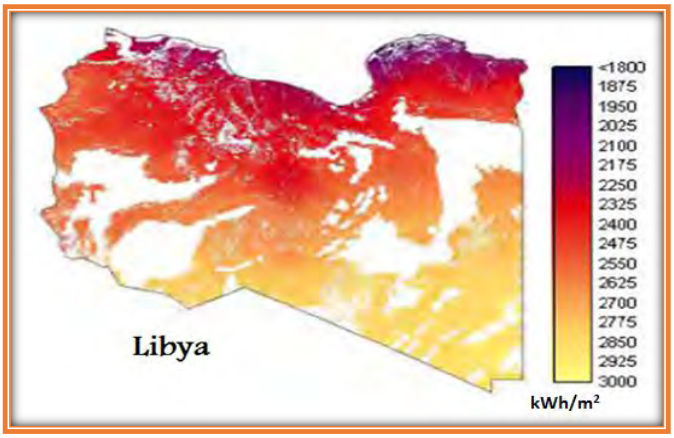

Figure 1:Average annual global horizontal radiation in Libya

1.2Water Supply Strategy in Libya

One of the most important problems nowadays, which is becoming more and more acute, is the scarcity offresh water of adequate quality for human consumption, and for industrial and agricultural use.Global demand for water continues to increase while freshwater sources are becoming scarcer due to increasing demand for natural resources and the impact of climate change, particularly in arid and semi-arid areas and coastal climates.

The global water demand is continuously increasing due to population growth and economic development. Global water withdrawals exceed 4,000 billion m^3 per year, and about 25% of the world population encounters fresh water scarcity [6].

According to the World Watch Institute, more than two-thirds of the world's populationmay experience water shortages by 2025. Thus, this

affects practically every country in the world, including the developed. This will occur unless they reducedemand and/or develop additional water sources.

1.3 Reverse Osmosis (RO)

This is a process in which salt water is pumped into a closed container against permeable membranes and forced to overcome the osmotic pressure of the salt solution. Hence, this technique requires a pre-treatment in order to be compatible with the membrane by removing suspended solids. This technique also needs a pH adjustment, which depends on the water source and the kind of membrane.

The technique is considered as the most promising one, and it can be used for both brackish and seawater desalination. It is used in a wide range of domestic sector without any need for additional chemicals. The system could be used for supplying the industrial sector if it was integrated within other thermal technology systems as shown in Figure 2.The use of RO desalination technology in Libya started in 1974at an average rate of 9200 m^3/d annually and a total installed capacity of over 140,000 m^3/d. Although most of the RO plants are used to desalinate groundwater, seawater desalination shares about 43% of the total installed capacity of all RO plants.

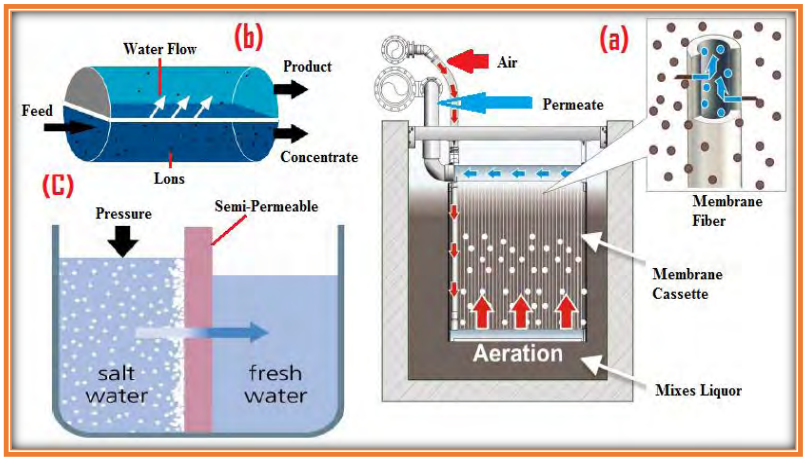

Figure 2: Assembly membrane (a), principle of ROdesalination (b) and, pressure forces water through the membrane(c)[7].

1.4 Solar PV Power Coupled with Desalination Technologies

Because of the negative environmental impacts of fossil fuels and the high cost of fresh water associated with desalination techniques using fossil fuels and natural gas, renewable sources such as solar energy have the potential to meet the national energy requirements in a sustainable way. Solar power is one of the most environmentally friendly ways to produce electricity, with no pollutant emissions and minimal environmental impact on the sites where it is installed. PV cells transfer solar energy directly into electrical energy, so no fuel is required.

In addition, PV panels are most often mounted on roofs and have practically no impact on land use.Libya needs to invest in solar energy seriously and effectively because of its vast area and geographical location with long periods of sunshine, clear skies, and the length of daylight hours, especially in desert areas. Added to that is the length of the coastline overlooking the Mediterranean and its proximity to the European Union

which gives Libya a great opportunity to export this energy to those countries.This project aims to establish a network of solar energy collection systems. Shown for PV cells below, PV power generation will be integrated into a grid connected to a power supply for reverse osmosis (RO) desalination plant,run by the RO system as shown in Figure 3.

The solar power is the best option and has flourished considerably in recent years due to technological advances.The main environmental impacts caused by seawater desalination include the following;

I. Seawater intake for desalination and for the cooling system may cause impingement and entrainment of organisms.

II. Chemical additives and biocides used to avoid fouling, foaming, corrosion and scaling of the desalination plants may finally appear in the brine.

III. Discharge of hot brine with high salt concentration to the sea may affect local aquatic species.

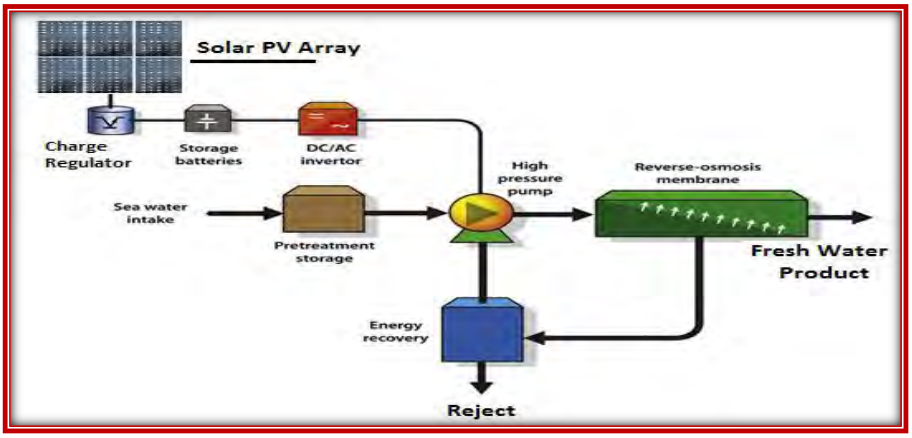

Figure 3: Scheme flow diagram of a PV–RO system [8].

2. Statement of the Problem

In this work we propose an economic study of a $50{,}000$ m^3/day reverse osmosis desalination plant powered by solar energy. The plant is designed for the remote area of Abutaraba, Libya, which falls in an area of very high isolation. The objectives of implementing this study are summarized as follows:

1) To analyze the data, design and calculate the necessary parameters and equipment needed to convert solar energy into electrical energy for the $8{,}500$ kWh/day seawater desalination plant in Abutaraba, Libya.

2) To evaluate the economic feasibility and compare the difference between the cost of freshwater when using fossil fuel energy and solar energy, in order to provide clean drinking water at the lowest cost.

3) To assess the environmental impact and the importance of protecting marine and coastal environment from pollution hazards.

2.1 Solar Power Potential in Libya

Libya needs to invest in solar energy seriously and effectively because of its vast area and geographical location, which gives a favorable climate, such as long periods of sunshine, clear skies, and the length of daylight hours, especially in desert areas where there is a high potential of solar energy which can be used to generate electricity by both solar energy conversions; photovoltaic, and thermal.

Added to that is the length of the coastline overlooking the Mediterranean and its proximity to the European Union which gives Libya a

great opportunity to export this energy to those countries. Hence, this study has been enriched by the studies carried out by some researchers in the field of desalination of sea water, solar energy and on the basis of the data measured by the Center for Solar Energy Studies and the General Electric Company of Libya (GECOL).

Solar power is renewable as long as the sun keeps burning the massive amount of hydrogen it has in its core, which at this point will be for another 4.5 billion years. Because photovoltaic (PV) uses this natural energy source, it does not require the mining, burning, or transportation of fossil fuels, which is why photovoltaic is considered to be a clean energy source.Basically, photovoltaic (PV) systems convert sunlight directly to electricity using the semiconductor materials in solar panels and the amount of power generated by a photovoltaic (PV) plant depends on the amount of direct sunlight at the site. Today's photovoltaic (PV) systems can convert solar energy to electricity more efficiently than ever before. Utility-scale trough plants are the lowest cost solar energy available today and further cost reductions are anticipated to make photovoltaic (PV) competitive with conventional power plants within a decade.

The production of photovoltaic (PV) is currently dominated by poly and mono-crystallinesilicon modules, which present 94% of the market and the other 6% include new technologies like thin films made of amorphous silicon or cadmium telluride and organicphotovoltaic.

This project aims to establish a network of PV cells to produce electrical energy, and PV power generation will be integrated into a grid connected to a power supply for reverse osmosis (RO) desalination plant,run by the RO system as shown in Fig (4).

On the other hand, the establishment of several desalination plants have the production capacity of 700 million m^3/year, and are processes that have been employed to provide water for industrial purposes since the 1960s [9].The technologies used on the industrial scale are generally classified into the following categories:

- ***Thermal Processes***

I. Multi-Effect Distillation (MED)

II. Multi-Stage Flash (MSF)

III. VaporCompression (VC)

- ***Membrane Technologies***

I. Reverse Osmosis(RO)

II. Electrodialysis (ED)

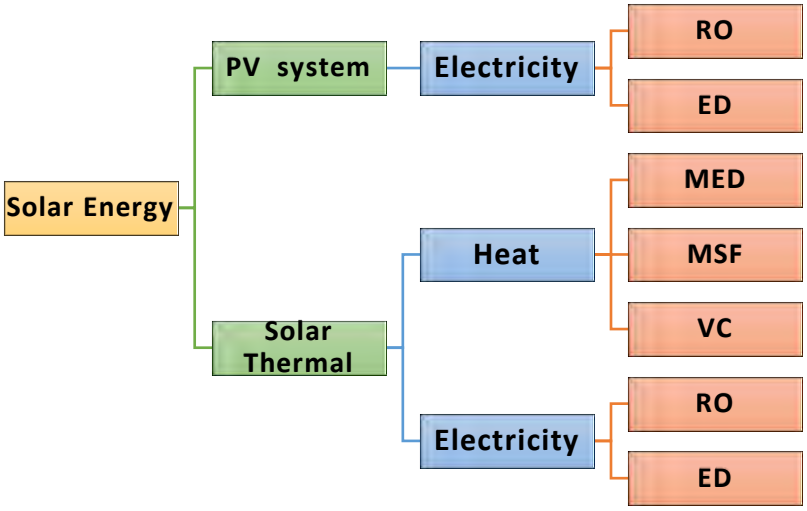

Figure4: Generally classified schematic of a PV–RO combinations system

2.2Quality of the Solar Radiation Falling on Libya

The location of the Abutarab plant in Benina is affected by the northeastern coastal climate that is hot and dry at summer with slight rain in winter. The data recorded by the Libyan Meteorological Department and Library of the Energy Resources Sector of the Center for Solar Energy Studies in Tripoli reveal a coastal arid climate a with high annual evaporation rate and a low annual precipitation rate.

The potential rate of evaporation in the coastal region is several times more that the average rainfall. Rain is rather sporadic, but it occurs very rapidly during a short time. Some rainwater infiltrates into the ground surface and percolates to recharge the aquifer, or is lost by water requirements for a community in a remote area in Abutarab.

The available data from meteorological and solar energy stations covering the period from1981−1988 were used to study and analyze the solar energy radiation on a horizontal surface in 11 stations covering the whole area of Libya. It is the only data presently available on Libya. Among the many models to choose from, we must choose optimal ones. These optimal ones take into account climate variables, such as relative humidity, maximum temperature, and cloud cover.

These climate variables have an important role in the amount of solar radiation which reaches the ground surface. This data can be used to estimate the solar radiation at the nearby locations, which are shown in Table 1.

station	Latitude	Longitude	Altitude(m)
Benina	32.1	20.15	39
Ejdabia	30.72	20.17	11
Elgariat	30.38	13.5	505
Gadames	30.13	9.5	331
Jagbub	29.82	24.32	3
Jalo	29.03	21.57	65
Nalut	31.87	10.98	626
Nasser	31.87	23.92	156
Sabha	27.02	14.43	437
Sirt	31.2	16.58	25
Tuburk	32.05	23.92	50
Tripoli	32.97	13.18	30
Shahat	32.82	21.82	626
Gat	24.95	10.17	699
Hon	29.13	15.95	265
Alkufra	24.26	23.3	408

Table 1: Shows location and altitude above sea level of the Libyan cities [10].

2.3Solar Radiation on the Surface of Inclination

The amount of solar energy falling on a horizontal surface changes as a result of the earth`s rotation and its movement around the sun. It is possible to provide data of the solar radiation falling on a horizontal surface and to calculate the optimal angles for as much solar energy as possible.

These angles are different from one place to another on earth and change depending on latitude and the changing seasons of the year. Since global solar radiation is a combination of direct solar radiation plus diffused solar radiation, we will first explain direct solar radiation.This is represented this by parallel solar rays that fall at an angle (i) which is verticalto the surface and is assumed to be inclined with a horizontal at an angle of (β), as shown in Figure 5.

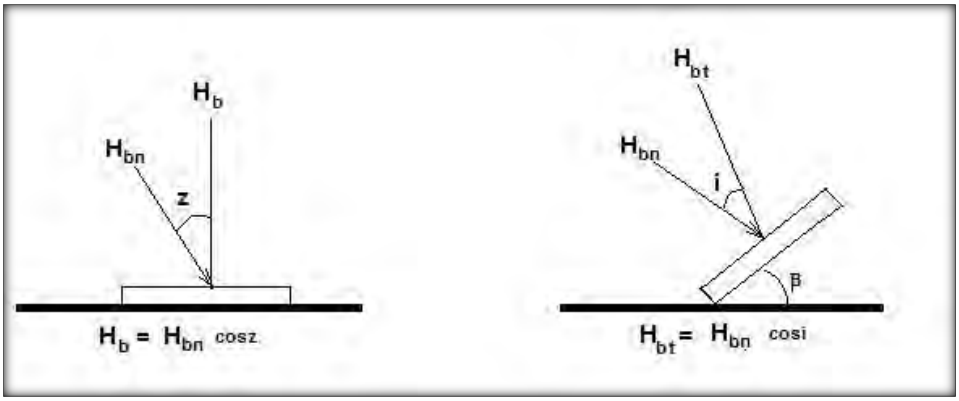

Figure 5: Direct solar radiation falling on surface of both horizontal and inclined surfaces

Assume that:

H_{bn} : Composite direct solar radiation falls on the inclined and horizontal surface

H_b : Composite direct solar radiation falls vertically on a horizontal surface

H_{bt} : Composite direct solar radiation falls vertically on the surface inclined at an angle *(β)* where horizontal *(β)* is the angle of inclination for the receiving surface.

It is possible to define (R_b) the coefficient inclination of solar radiation as a direct ratio between the direct radiation falling on the surface of the slant and that which is falling on a horizontal surface in the northern hemisphere[11]

.

$$R_b = H_{bt} / H_b = \cos i / \cos z \text{ ----------(1)}$$

In the southern hemisphere, we find that:

$$\cos i = \sin(\phi - \beta)\sin\delta + \cos(\phi - \beta)\cos\delta\cos\omega \text{ ----------(2)}$$

$$\cos z = \cos\phi\cos\delta\cos\omega + \sin\phi\sin\phi \text{ ----------(3)}$$

2.4 Estimate of Solar Radiation on Inclined Surfaces and Optimal Angles

Liu & Jordan [12] was the model used to calculate optimal angles monthly, using the data of solar radiation on a horizontal surface. The model assumes that the diffused radiation is radiation homogeneous to the celestial dome, and this means that the amount of diffused radiation that the surface receives depends on the part of the surface which faces and is surrounded by the sky. We find here the inclined surface with the horizontal angle (β) facing the sky, which gives the relationship *(1+ cos*

$\beta)/2$. Accordingly, the amount of diffused radiation received by this surface is $H_d\ (1+\cos\beta)/2$ where H_d is the level of composite diffuse radiation falling on a horizontal surface.

This inclined surface also receivesradiation reflected from the surface of the earth and surrounded by other objects,on the assumption that this is the medium of reflectivity (P) between direct and diffuse radiation. Thus, the amount of radiation reflected from the ground, the surrounding atmosphere,and falling on the surface of the inclined angle (β) will be equal to $p\ (1+\cos\beta)/2$ of the total radiation which is equal to ($H_d + H_b$).

However, we find that the total radiation on the surface of the receiver in the inclined angle (β) will be the sum of direct radiation, diffused radiation, and radiation reflected by the relationship:

$$H_t = H_b R_b + H_d(1+\cos\beta)/2 + (H_b + H_d)p(1-\cos\beta)/2 \text{ ------(4)}$$

This is where (H_t) is the amount of total radiation falling on the inclined surface. This formula is named Liu & Jordan. Thus, the coefficient of the inclination of total solar radiation is as follows:

$$R = H_t/H = H_b/H \quad R_b + H_d/H \quad (1+\cos\beta)/2 + p(1-\cos\beta)/2 \text{ ----(5)}$$

This formula can be used to find the values of solar radiation hourly, daily, or monthly in terms of importance in different applications. This is the case of although the monthly average solar radiation becomes most important in the design of solar systems.

Therefore, the equation that gives the average is the following:

$$\bar{R} = \bar{H}_t / \bar{H} = (1 - \bar{H}_d / \bar{H})\,\bar{R}_b + \bar{H}_d (1 + \cos\beta)/2 + P(1 - \cos\beta)/2 \quad \text{.....(6)}$$

Where:

$\bar{H}_T$ is the average monthly amount of total solar radiation falling on the inclined surface

$\bar{H}$: is the average monthly amount of total solar radiation falling on a horizontal surface.

R_b : Monthly average of the direct inclination.

β: Inclination angle of the receiving horizontal surface

P:Reflectivity of the earth which Liu & Jordan suggested as being limited to a value between 0 and 1.

Where (R_b) is a function of complex permeability in the atmosphere, except at the equinoxes and thus is dependent on the purity of the atmosphere in terms of both the amount of water vapor and the concentration of particles in the atmosphere.

There are two ways to account for the surface of the southern hemisphere facing the northern hemisphere. The Liu& Jordan model gives the following relationship:

$$\bar{R_b} = \frac{\cos(\phi - \beta)\cos\delta \quad \sin\omega_s \quad + \quad (\pi/180)\omega_S` \quad \sin(\phi - \beta)\sin\delta}{\cos\phi \quad \cos\delta \quad \sin\omega_s \quad + (\pi/180)\omega_s \sin\phi \quad \sin\delta} \quad \text{.....(7)}$$

Where ω_S` is the angle of the hour of sunset on the surface of the slant in degrees and is equal to the following:

$$= \sin \begin{bmatrix} \cos^{-1} & (-\tan\phi \tan\delta) \\ \cos^{-1} & (\tan(\phi-\beta)\tan\delta \end{bmatrix} \text{.....(8)} \ \omega_S`$$

These results were obtained from Liu& Jordan and show the rate of monthly total solar radiation falling on the inclined surface as a function of the angle of inclination of the different sites.

2.5 Climate of Benina City and Solar Data

The available data from meteorological and solar energy stations covering the period of $(1981-1987)$ were used to study and analyze the solar energy radiation on a horizontal surface in 11 stations in Libya.

One of those stations is in Benina at Lat of a $32^0.10$ N this location was chosen for this research about 100 km west of the latitude of the Abutraba RO desalination plant. The monthly average solar radiation in the south facing tilted surfaces has also been calculated for the location using the solar radiation data available for a horizontal surface.

The measurements show that the maximum rate of solar radiation ranges from 9.30 to 10.69 kWh/m^2/day, while the annual average per year is between 5.79 to 8.58 kWh/m^2/day [13], with average sun duration of more than 3500 hours per year. The constants used in the analysis are given in Table 2.

Parameters	Value
Location	Benina City
Latitude	$32^0.10$ N
Longitude	$20^0.15$ E
Maximum solar radiation	10.69 kWh/m^2/day
Peak radiation	1040 W/m^2
Average solar radiation	8.58 kWh/m^2/day
Average sun duration	3500 hours/yr
Maximum daylight hours	12.50 hours
Minimum daylight hours	5.4 hours
Average daylight hours	9.25 hours
Average temperature	26 ^{0}C

Table 2: Input parameters of available energy data analysis for PV

Designing and utilizing solar radiation data (global, diffuse and direct) require some meteorological variables. Figures 6, 7 and 8 show the mean monthly sunshineduration (hours), mean monthly cloud amount, the

(maximum, mean and minimum monthly ambient temperature), as well as the (mean monthly relative humidity % and mean wind speed).

All of this data was obtained from the Libyan Meteorological Department and the Library of Energy Resources Sector for Solar Energy Studies in Tripoli [14]. From this data, it appears that the site`s climate conditions are convenient for solar energy production.Figure 6 shows the change in the brightness of sun hours per month and per year. In Benina City, the number of hours of brightness gradually increases beginning in January until it reaches the month of July.

Atthis time, the hours of brightnessgradually decrease. Thus, the more clouds in the sky, the less direct solar radiation there will be.

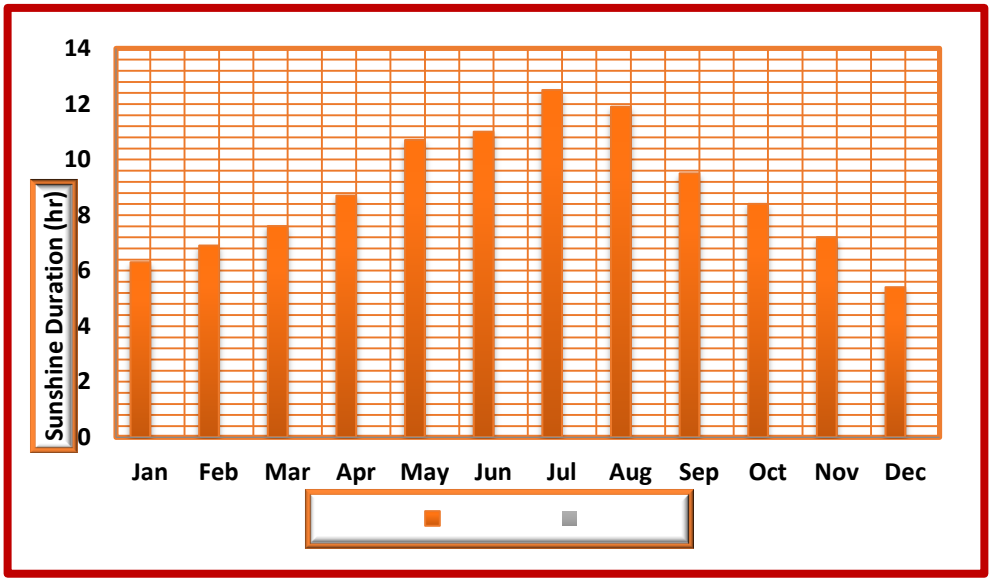

Figure 6: Monthly mean sunshine duration hours and monthly in Benina City

From Figure 7, the change in average monthly temperature starts to gradually increase with the month of January until it reaches stability for the months of May, June and July. It then begins to decline again until the month of December. However, the temperature is the main manifestation of solar energy. It can be done by comparing the temperature with solar radiation. That there is a similarity in the monthly change of temperature and the amount of solar radiation that reaches the city. Once all other factors have been installed, the temperature can be an indicator of increased or reduced solar energy.

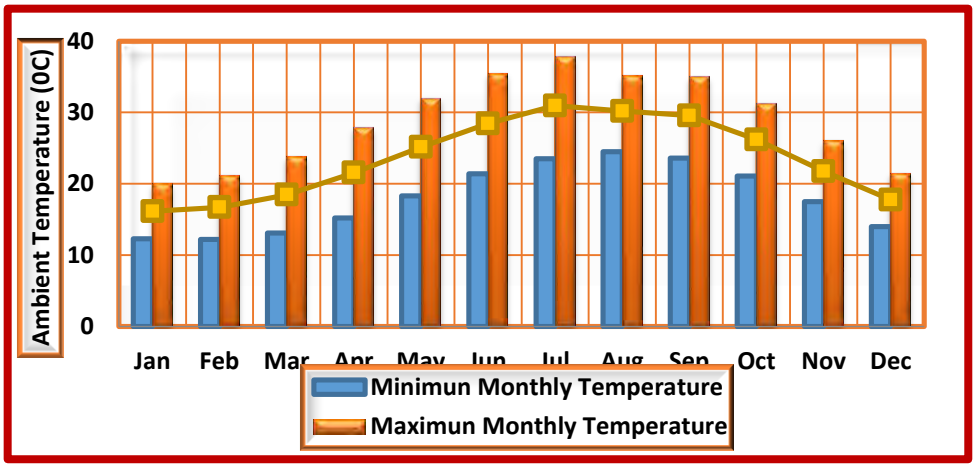

Figure 7: Average daily min, mean and max temperatures (°C) in Benina City

In Figure 8, the change in average monthly relative humidity gradually increases starting in November and continues until March, which is when it then declines until October. Therefore, this shows that the less humidity and wind speed there is, the more solar radiation there will be.

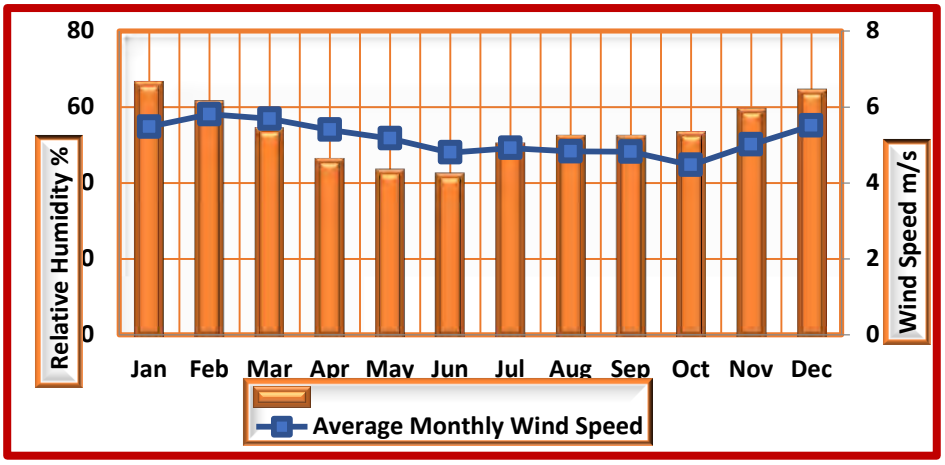

Figure 8: Monthly average relative humidity and wind speed in Benina City

3. Results and discussion

3.1 Calculations *of Solar Radiation on a Horizontal Surface*

Many models have been used to predict the amount of solar energy evident on a horizontal surface. One of the simplest methods is the well-known Angstrom Correlation Duffie and Beckman from 1991.

It gives the smallest percentage error for the estimation ofdaily global solar radiation, which can be written in the following form.

$$\bar{H} = \bar{H`}_0 (a + \frac{b\bar{n}}{N}) \ldots\ldots\ldots\ldots\ldots\ldots (9)$$

$\bar{H}$: is the monthly average of daily global solar radiation on a horizontal surface (kWh/m^2/day)

$\bar{H`}_0$: is the extraterrestrial solar radiation on a horizontal surface on an average day of each month (kWh/m^2/day)

$\bar{n}$: is the monthly mean daily number of hours of observed bright sunshine

$\bar{N}$: is the mean daily number of hours of daylight in a given month between sunrise and sunset, and (a) and (b) are regression coefficients.

Where:

$$N = (\frac{2}{15})\omega_s \text{.....(10)}$$

$$\omega_s = \cos^{-1}[-\tan\phi\tan\delta] \text{.....(11)}$$

$$H_o = \frac{24 I_{sc}}{\pi}\left[1 + 0.033\cos(360\frac{\bar{n}}{365}\right] \times \left[\cos\phi\cos\delta\sin\omega_s + \frac{\pi\omega_s}{180}\sin\phi\sin\delta\right] \text{.....(12)}$$

$$\delta = 23.45\sin\left[360(284 + d)/365\right] \text{.....(13)}$$

I_{sc} (the solar constant)= 1.367 kW/ m^2, ω_s is the sunset hour angle in degrees, δ is the declinationangle, d is the average amount of daylight for the given month, and ϕ is the latitude angle in degrees.

The average values of $(\bar{H}/H_0)$ and $(\bar{n}/\bar{N})$ for the period from 1981 to 1987 for each month are computed for Benina City and are displayed in Table 3. Rietveld [15] suggested values for the constants (a,b) in the AgeströmModel [16].

The atmosphere and geographic variables linked to the proportion of sunshine hours are as follows:

$$a = 0.1 + 0.24(\bar{n}/\bar{N}) \text{ ..... (14)}$$

$$b = 0.38 + 0.08(\bar{N}/\bar{n}) \quad \text{..... (15)}$$

If these values are placed in equation (8), we find:

$$\bar{H}/\bar{H}_0 = 0.18 + 0.62(\bar{n}/\bar{N}) \quad \text{.....(16)}$$

Month	*Average values of* $(\bar{\bar{H}}/H_0)$	*Average values of* $(\bar{n}/\bar{N})$
January	**0.514**	**0.594**
February	**0.529**	**0.593**
March	**0.565**	**0.643**
April	**0.593**	**0.664**
May	**0.587**	**0.71**
June	**0.612**	**0.832**
July	**0.635**	**0.861**
August	**0.626**	**0.866**
September	**0.628**	**0.82**
October	**0.581**	**0.766**
November	**0.546**	**0.659**
December	**0.448**	**0.606**

Table 3: Shows average values of $(\bar{\bar{H}}/H_0)$ and $(\bar{n}/\bar{N})$ for the period (1981 to 1987)

Only seven years of monthly average global radiation data is available for Benina city. A reliable model for estimating solar radiation is not obtainable for each single month; so, to increase the number of data points, the monthly data was merged together to produce 96 data points for each station. The regression equations obtained are given in Table 4.

Station	Latitudeϕ	Number ofmonth	Intercept (a)	Slope (b)	CorrelationCoefficient(R)
Benina city	32^0.10'N	84	0.350527	0.319205	0.571125

Table 4: Shows values (a) and (b) in the regression equation:

$$\bar{H}/\bar{H}_0 = a + b(\bar{n}/\bar{N})$$

Direct solar radiation, diffused solar radiation, and global solar radiation have been drawn in the form of histograms, and these forms represent the average monthly radiation of the three different kinds falling on a horizontal surface. The city of Benina was chosen because it is close to the station site. Figure 9 shows the annual change of solar radiation falling on the city of Benina.

There is a change of total solar radiation from 3.68 to 10.69kWh/m^2/day, with a monthly rate of 83.6 % of solar radiation entering from outside the atmosphere, and direct radiation representing about 79 % of the total radiation.

It is clear that, in general, the values of the total radiation falling on a horizontal surface in Benina City are characterized by a rise during the year, especially in the months of May, June, and July. In comparison, it is low in the months of December and January.

Therefore, it can be said that the annual rate of change from 4.44 kWh /m^2/day to 10.69 kWh /m^2/ day during the year equals the average total amount of solar radiation.

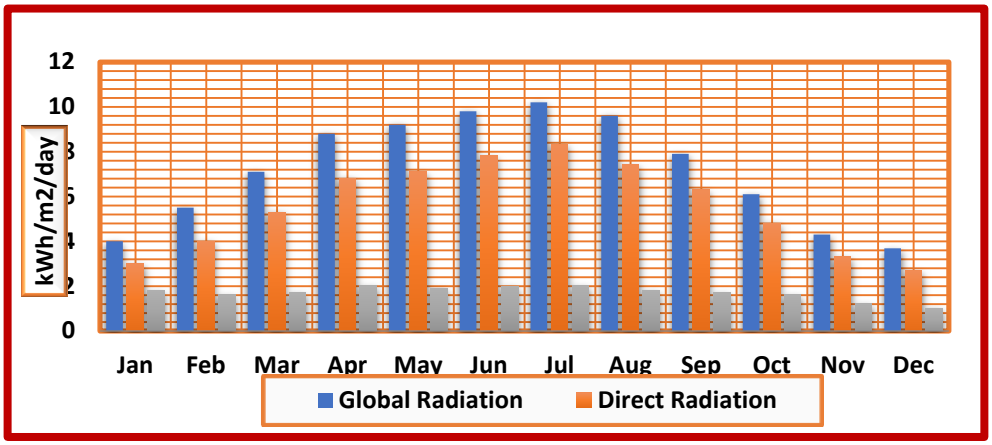

Figure 9: Solar radiation falling on a horizontal surface in Benina City

3.2 Designing of a PV– RO System for the Abutraba Plant

The system basically consists of a seawater RO desalination plant operating and an isolated photovoltaic system PV with power storage based on batteries and production of the power requiredfor the desalination process.

The major factors influencing the electrical design of the solar array are asfollows:the solarpowerintensity, the sun optimum tilt angles and the size of solar array.

In order to design the PV-RO system, the 280,000 kW PV arrays have been modeled on conditions pertaining to a RO desalination system in Abutraba producing 50,000 m^3/d. Temperature is an important effect on the output and efficiency of the PV power, with the optimum tilt angle, sunshine hour duration per day and PV array modules evaluated for a potential plant location as displayed in Table 5.

Technical Parameter	*Unit*
Mean solar radiation	**2010 kWh/m^2/year**
Sunshine duration	**350 d /year**
Production water capacity	**50,000 m^3/day**
Energy required for RO plant	**250,500 kWh/day**
Energy design from solar PV	**280,000 kWh/day**
Cell efficiency [9]	**16.5 %**
Plant lifetime	**25 years**
PV Module efficiency	**16.8%**
PV cell temperature [9]	**70 ^{0}C**
Mean annual humidity	**67%**

Table 5: Site-specific analysis data and next steps for a RO-PV system

The sizing and design of a PV cell system using 280,000 kW PV array solar power is needed to run the RO desalination station. The solar module is the heart of the whole PV system and the solar module is composed of several individual PV cells connected in series or parallel. The cells can be arranged in a module to produce a specific voltage and current to meet the particular electrical requirements.

The area of horizontal PV arrays needed is important because it is proportional with output voltage of the PV cells, and it defines the requirement of the field area for the PV array and RO desalination plant.

Also, the PV solar array is the first step estimating the cost for PV solar arraysystems. The efficiency of PV power cells is based on commercial availability.

3.3 System Design of PV Area Size

The proposed280,000 kW/day PV power plant would be divided into 280 substations of 1000 kW each, and each 1000 kW substation would be divided into five channels rated at 200 kW. Each substation would feed the generated electricity to the 400V/11 kV/1MVA grid through a 1000 kVA transformer, and each 200 kW PV channel has been equipped with a grid-connected inverter to convert the DC power from the PV into three-phase AC power for the 1000 kVA transformer. The output from the 280,000 kW station connects to the national grid (240 kV) through a 280,000 kVA transformer. The configuration of the basic array consists of 25 modules, five modules in series, and five series in parallel. Forty basic arrays make one 200 kW PV substation, connected to one inverter with the array unit consisting of 5000 modules.

The schematic is identical to a simple schematic design of the photovoltaic reverse osmosis system considered, which is shown in Figure 10. In this system, the energy source is the photovoltaic power system or the diesel generator / electric generator, powers a feed pump and a high pressure pump to provide pressure to the incoming water.

The water is then driven through the RO membrane array by the high pressure produced by the pumps, leaving high salt concentration brine on one side and low salt concentration water on the other side. The high pressure brine stream passes through a turbine to recover its energy before exiting the system.

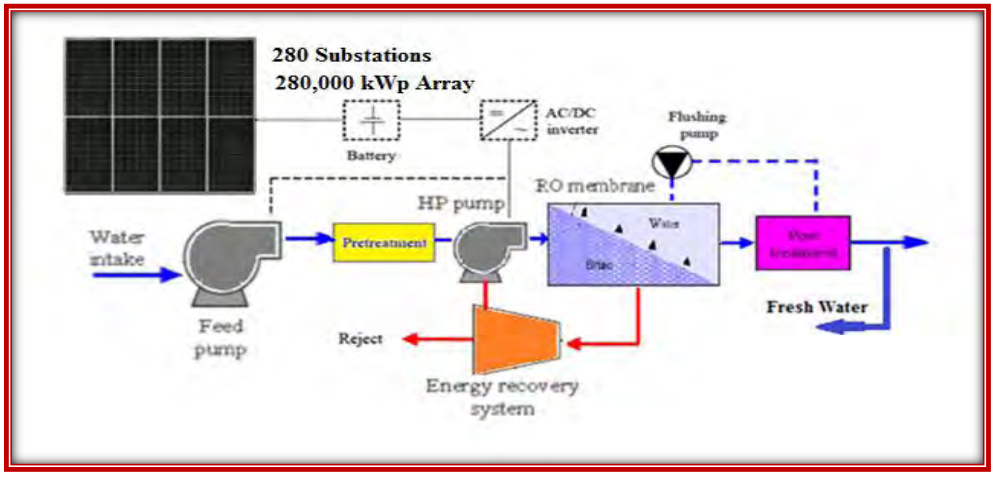

Figure 10: Simplified general design schematic of a PV–RO desalination system

3.4 Typical Solar PV Cell Power Field

The PV modules have been fixed so that they do not shade each other; thus, only the sun's apparent motion across the sky needs to be taken into consideration in order to optimize the spacing between rows of modules.

Figure 11 shows the configuration of the basic array whose dimensions are 6.59 m in length and 4.4 m in width. To avoid any shadowing, the distance between the PV sub-arrays is 6 m, which has been calculated from Equations (21 and 22) [17].

$$\frac{d}{a} = \cos\beta + \frac{\sin\beta}{\tan\varepsilon} \quad \text{.....(17)}$$

Where (β) is the tilt angle, (ϕ) is latitude angle and (ε) can be estimated by the geographical latitude (ϕ), (δ) which is the declination angle given by:

$$\varepsilon = 90 - \delta - \phi \quad \text{.....(18)}$$

$$\delta = 23.45\sin(360\frac{284+n}{365}) \quad \text{.....(19)}$$

The (n)represents the day of the year. Equation (23) can be used to obtain the cos θ_z = zenith angle:

$$\cos\theta_z = \sin\phi\sin\delta + \cos\phi\cos\delta\cos\omega \quad \text{.....(20)}$$

The value of (ω) is given by:

$$\omega = 15(hr - a) \quad \text{.....(21)}$$

Where a = 11.75, at which ω = 0 and hr = solar local time and the value of (hr) can be obtained from the following:

$$hr = \text{standard} + 4(L_{st} + L_{loc}) + E \quad \text{.....(22)}$$

Where L_{st} = standard meridian for the local time zone, L_{loc} = longitude of location.

The value of E can be obtained fromthe following:

$$E = 9.87\sin 2B - 7.53\cos B - 1.5\sin B \quad \text{.....(23)}$$

Where $B = 360(n-81)/365$.

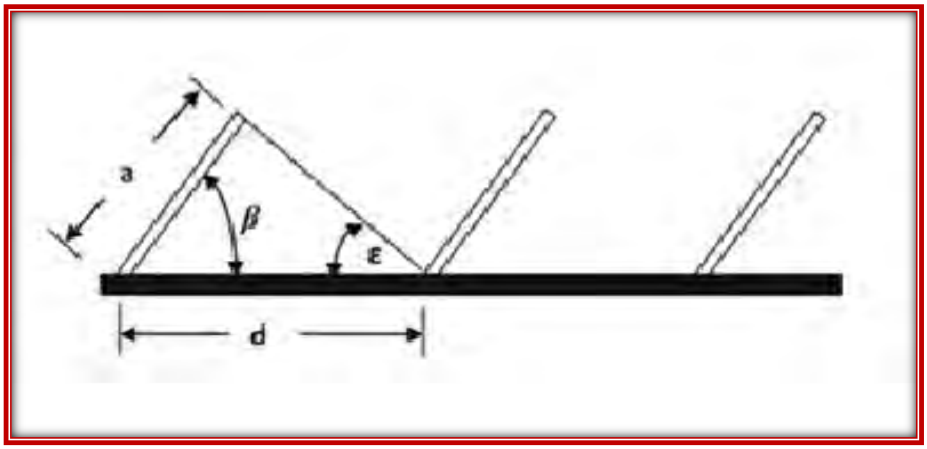

Figure 11: Arrangement of a large number of rows of basic array

The area required for a 280,000 kW PV substation is the following:

length = 969 m X Width = 2356.5 m, which is = the total area of 2234998.5 m^2.

For a proposed image, a 280,000 kW PV system and its corresponding analysis result from a PV area, as is shown in Table 6, this data has been calculated by Kurokawa and Keiichi [18].

Parameter	***Value***
Latitude angle (ϕ)	**32.10^0**
Tilt angle (β)	**29.17^0**
Declination angle (δ)	**0.45^0**

Zenith angle (θ_z)	0.5^0
Longitude of location (L_{loc})	20.15^0
Module area	29 m^2
No. of Modules	1,400,000
Solar cells area	2,234,998.5 m^2
Total area of PV substation	2,962,120.5 m^2

Table 6: Specification analysis results of the proposed PV area

4. Conclusions

4.1 Assessment *of the PV-RO System*

As mentioned at the beginning of this project, Libya has serious water shortage problems due to the fact that most of Libya is located in arid and semi-arid zones known for their scanty annual rainfall, very high rates of evaporation and consequently extremely insufficient water resources. Sustainable management of water resources is vital because water scarcity is becoming more and more a development constraint impeding the economic growth in Libya. Arid areas, with their many inhabitants, need a continual source of fresh water. It is difficult for the utility network of electricity to reach these areas.

It is also difficult to transport fuel to diesel engine sets of large sizes. For these reasons, it was essential to find a solution for such a problem. The future vision of Libya in the field of desalination is to be based on solar PV cells. This is due to the fact that solar PV seems to be a good

solution for such projects. This solution is dependent upon the meteorological data in these areas. A PV can be very useful in areas where high solar radiation is abundant over the whole year.

The environmental benefits can be added to the advantages of these methods.In this case, we present an economic feasibility study on a $50{,}000$ m^3/day RO desalination plant with alternative powering systems. The solar PV cell is designed for remote areas in Abutrab-Libya, which falls in an area of very high radiation. This city also lies in the so-called solar belt with an average solar radiation of 8.58 kWh/m^2/day.In the process, it can be concluded that the study sheds light on the following points:

- An RO plant fully driven by solar PV used,RO plant production has a water capacity of $50{,}000$ m^3/day and energy design from solar PV has a capacity of $280{,}000$ kWh/day in contrast, the energy required for an RO plant is $250{,}000$ kWh/day.

- The global solar radiation varies between a minimum of 3.68 kWh/m^2/day at Benin and a maximum of 10.69 kWh/m^2/day while average value remained as 8.58 kWh/m^2/day.

- The duration of maximum daylight hours was at 12.50 hours with an overall average of 9.25 hours or about a total of 3500 hours in a year.

- The mean value of cost of electricity from solar PV was found to be $0.5 - 0.7$ US$/$m^3$ while thetotal solar PVarray system cost 42 million US$ on economic indicators. Benina was found to be the best site for the development of a solar PV based power plant.

- An RO plant powered only by solar PV power. Plant equipmentis sized so that the water demands for the 24 hours, and is produced during sunshine hours.In addition, a battery-assisted PV-RO plant is used to drive the RO plant during night or blackout hours.

It is clear that it is important to find the amount of solar radiation falling on the collection of solar cells at the inclination angle. Through the study and calculation of the optimum angles for Benina,the following can be concluded:

1. To collect the highest amount of solar energy during the summer, May, June, July for all models such as (All sky model) and Hay, Davies, Klucher and Rrindal (HDKR model) of Benina, the collection of solar cells must be installed in a horizontal position.

2. To collect solar energy during the highest amount of annual radiation, a fixed angle of Benina and the models, as well as the collection of solar cells, must be installed at an angle equal to the latitude facingsouth.

For angles using the declination angle and zenith angle:

3. To collect the highest amount of solar energy during the summer, install solar cells ata declination angle of $23^0$and zenith angle of 12.5^0.

4. To collect the highest amount of solar energy during the winter, install solar cells at a declination angle of $-23^0$and zenith angle of 7^0as shown in Figure 12.

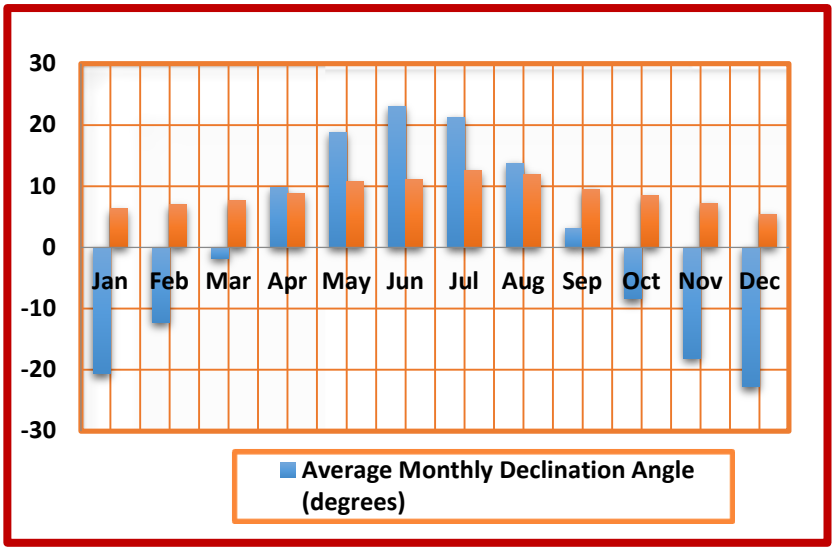

Figure12: Monthly average declination angle and zenith angle in Benina City

In this case, Benina possesseslatitudeof a $32^0.10$ N where the solar PV arrays are installed. It is found that the optimum tilt angle changes throughout the year. In the winter, December, January, and February the tilt should be 55^0, in the spring, March, April, and May the tilt should be 17.5^0, in the summer June, July, and August the tilt should be 3.5^0, and during autumn September, October, and November the tilt should be 40.5^0 as shown in Figure 13. The yearly average of this value was found to be 29.17^0 which is nearly the same as the latitude of Benina, which was found to be $32^0.10$ N. This, in general, corresponds with the results of many other researchers.

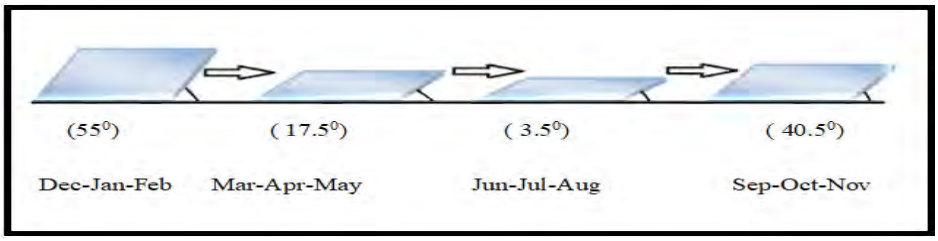

Figure 13: Seasonally adjusted tilt angles

Specific energy consumption rates for desalination plants are decreasing continuously due to advances in technology and the use of energy recovery devices. The value for specific energy consumption can be as low as 3 kWh/m^3 for new plants. For the reason, which number was used for the estimation of unit production costs for different types of energy as shown in Figure 14.

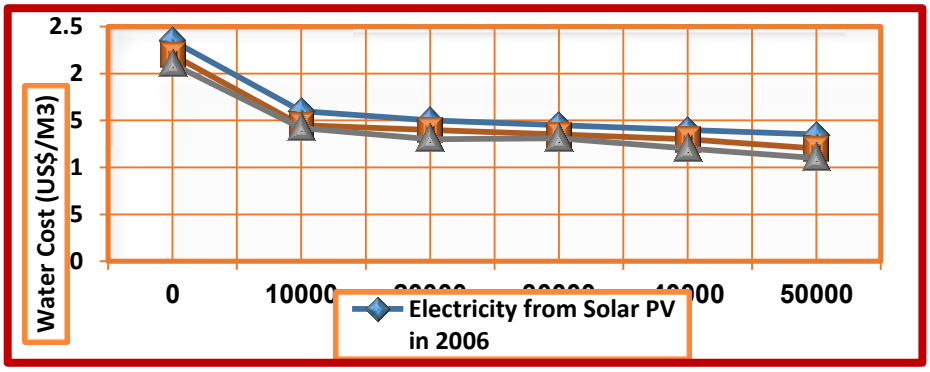

Figure14:Water cost as a function of the plant capacity of electricity from the solar system and fossil fuels

4.2 Economic Feasibility

This dependency is due to the differences in terrain characteristics, as well as the difference in bout solar resources and water characteristics. For the conditions analyzed, the PVRO is feasible for many water deficient

regions. The high fuel costs for the diesel powered systems result in higher water costs for most locations.

When the system is configured for a region without good solar resources, the high capital costs for community scale seawater PVRO systems are not recovered during the system`s lifetime. With modular design methodologies and intelligent system control of the PV powered RO systems, it is possible that the system costs could be further reduced, and the PVRO systems could become affordable for larger areas. This method compares the cost of water producedPVRO to water producedelectricity from diesel-powered RO.

The energy requirements are then used to determine the water cost for each system. A PVRO system is considered feasible since it is more cost effective than an equivalent diesel based system. Today, the costs for each source of electricity generation cannot facilitate the choice between either PV or CSP since they lie very close to each other. Moreover, if PV prices keep falling as they started to do so in 2009; it is very likely that PV takes the lead in terms of electricity generation costs within the next decade.

Nevertheless, the CSP technology brings an important dimension to energy quality by allowing a stable output throughout the day and energy storage during the night. This is certainly a major advantage in countries where the consumption peak occurs during evening hours. However, the implementation of storage results in very high investment costs, which might not necessarily be justified by the energy advantage.

The solar PV modulehas been used in this study among the analyses PV modules due to its high efficiency and large module capacity. The results confirm that Libya has a high content of annual solar radiation. The collected meteorological parameters were long-term daily global radiation, daily sunshine hours, and long-term hourly ambient temperature.

By usingMicrosoft Excel program have been constructed to compute slope radiation, the optimal tilt angle degree in Benina, as well as maximum solar PV power output, and module efficiency for the solar PV system, as shown in Table 7.

Technical Parameter	Unit
Production water capacity	50,000 m^3/day
Energy required for RO plant	250,000 kWh/day
Energy design from solar PV	280,000 kWh/day
PV Module efficiency	16.8%
PV cell temperature [9]	70 ^{0}C
Total area of PV substation	202653 m^2
Cost of Production water from Solar PV/RO	0.5 – 0.7 US$/$m^3$
Cost of electricity from Solar PV	0.45 US$/kWh

Table 7: The cost of water produced using PVRO

5. Recommendations

Finally, the data gathered during this study has led to some very promising results. To further validate and improve upon the findings of this study, it is recommended to use PVRO plants atLibya without any delay. Solar PV is considered as one of the cleanest sources of energy available today. The most significant feature of solar energy is that it does not harm the environment.

It is clean energy asusing solar power does not emit any of the extremely harmful greenhouse gases that contribute to global warming. Additionally, in light of the necessity to tackle climate change, energy produced from renewable sources is gaining importance. Solar PV power technologies with promising low carbon emissions will play an important role in the supply of global energy in the future.

Solar PV power projects have the potential to compete with conventional power generation sources in the near future. In Libya, if the government is to shift towards centralized desalination plants in the future to tackle increasing water shortage, this would favor the adoption of solar PV as a more economic and climate friendly energy source.

References

[1] World Health Organization and UNICEF, Meeting the MDG drinking water and sanitation target, 2006, http://www.who.int/water_sanitation_health/monitoring/jmpfinal.pdf, accessed April 3, 2009.

[2] Alfenadi Y. Hottest temperature record in the world, El Azizia, Libya, 2007.

[3] Dr. Franz Trieb.," Concentrating Solar Power for Seawater Desalination", Menarec 4, damascus, syria, june 20-24, 2007.

[4]. Eljrushi, G.& Veziroglu, T. N., "Solar-hydrogen energy system for Libya".Int. J. Hydrogen Energy, 15 (1990) 885-94.

[5]. Fichtner,2011, MENA Regional Water Outlook Part II Desalination Using Renewable Energy. Fichtner, Germany.

[6]. Rosegrant, M.W. et al., 2002, Global Water Outlook to 2025, Averting an Impending Crisis, International Food Policy Research Institute and International Water Management Institute.

[7]. O.K.Buros. The desalinating ABC, McGrawhill, New York, 1990.

[8] Maurel A. Desalination by reverse osmosis using renewable energies (Solarwind): cadarache central experiment. In: Proceedings of the new technologies for the use of renewable energy sources in water desalination conference, session II, Athens, Greece; 1991. p. 17–26.

[9] Elkhlat M. Energy Efficiency and Renewable Energy Libya National study. General Electric Company of Libya (GECOL) 2007.

[10]. Information Department, 81-87 "Average of Solar Radiation Measurements". Center for Solar Energy Studies, Tripoli, Libya, 1988.

[11]. Liu, R.Y. and Jordan, R.C, 1960, "The Interrelationship and Characteristic Distribution of Direct, Diffuse and Total Solar Radiation", Solar Energy, 4(3), 1-19.

[12] Amer, A. M., 1992, "Measurement and analysis of global and diffuse solar radiation of Tripoli Libya from sep.1989-1990", M. Sc. Thesis, Department of physics.

[13] Amer, A. M., 1992, "Measurement and analysis of global and diffuse solar radiation of Tripoli Libya from sep.1989-1990", M. Sc. Thesis, Department of physics.

[14] Shakshouki, F. H. et.al., "1981-1987 Average solar radiation measurements", Information and Computer Section, Center for Solar Energy Studies, Tripoli, Libya.

[15] Klein, S. A., 1977, "Calculation of monthly average insulation on tilted surface", Solar Energy, 19, 325-329.

[16] °Angstrom, A., 1924, "solar and terrestrial radiation", Q. J. Roy. Met. Sec,50, 121-126.

[17] Goetz A, Hoffmann V. Photovoltaic Solar Energy Generation. Springer, 2005.

[18] Hoffmann, W., 2006. PV solar electricity industry market growth and perspective. Solar Energy Materials and Solar Cells 90, 3285–3311.

Journal of Total Science
Volume (6), Issue (23) March. 2023)
ISSN: 2518-5799

مجلة العلوم الشاملة
المجلد (6)، العدد (23)، (مارس2023)
ردمد: 2518-5799

Wavelet Transform and Entropy An overview of radioactive radon gas

Aliya M Kishada

University of Zawia – Zuwara Faculty of Education – Physics Department

Abstract:

This paper aims to introduce the deadly radioactive radon gas as the most important natural radioactive source in the environment and its risks to human health. in addition to the importance of measuring its concentrations in the environment. As well as some health effects resulting from exposure to different doses of this deadly gas and ways to protect ourselves against it. Sources of this deadly radioactive radon gas are also presented in this paper.

Key words: radon, radon risks, radon indoors.

1- Introduction:

It is universally known that lung cancer is a public health problem and the number one cause of cancer death worldwide [1,2]. In addition, the number of lung cancer cases among non-smokers has increased in recent years. The ionizing environmental radiation represents a major epidemiological concern world - wide, with radon representing the main risk factor of lung cancer in non-smokers and the second factor in smoking patients, with synergistic effects in the latter. Radon leads to DNA damage and high genomic tumor instability, but its exact carcinogenesis mechanism and relationship with lung cancer remains unknown. It is time for more studies about radon to know its mechanisms of cellular damage, its potential long-term health consequences and its undeniable relationship with lung cancer.

We hope that the ongoing studies will provide new data on the role of indoor radon exposure in the molecular signature of lung cancer, especially in non-smokers, as well as in the clinical and biological characteristics of lung cancer. These studies will strengthen scientific knowledge on lung cancer carcinogenesis, providing relevant information on how radon affects the evolution of lung cancer and if there is any impact on its prognosis. They will also contribute to promoting radon policies and strategies on cancer prevention.

2- Radon Characteristics:

It is well known that radon (^{222}Rn) was first discovered by Dorn in 1900 [3]. Radioactive radon gas is an invisible, naturally occurring, colorless, odorless, radioactive gas that causes cancer and is found in rock, soil, water and some building materials. Table (1) below shows some properties of this element.

Table 2: Properties of radon-222

Atomic weight	222
Atomic number	86
Half life	33.8 days
Boiling point	62.1 °C (760 mmHg)
Density	9.73 g l1 (0 1 C, 760 mmHg)
Melting point	71.1 °C (760 mmHg)
Critical pressure	62 atm
Critical temperature	104.1 °C

Radon is a natural radioactive gas that has a direct effect on human health [4]. It has been identified as the first leading cause of lung cancer.

Radon-222, with a radioactive half-life of 3.8 days, is the main radon isotope of health concern. It is released during the decay of uranium-238 and subsequently radium-226, which are found in varying amounts in the indoor air, rocks, soils and groundwater. Radon gas cannot be detected with the human senses. But often is substantially concentrated indoors because homes are not normally built to be radon resistant. The potential for radon exposure varies by geographic area; however, even buildings constructed in areas considered to have low radon potential can exhibit greatly elevated radon concentrations. This dangerous radioactive gas comes from the breakdown of naturally occurring radium-226 found in soils and rocks that surround the foundations of our homes and work places. Figure (1) shows the sources and average distribution of natural background radiation for the world population. It is well known that human exposure to radioactivity comes mainly from natural sources, radon and its progeny breathed in the air being responsible for more than 50% of the annual dose received from natural radiation [5].

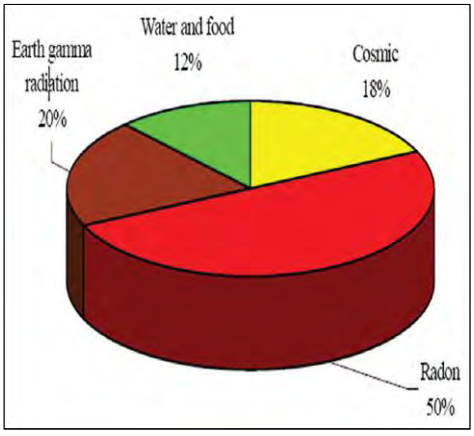

Fig 1. Distribution of natural background radiation for the world population [5].

3 – Radon indoors:

Indoor radon concentrations vary from country to country and even between different buildings due to differences in climate, building techniques, available ventilation methods, household habits, and most importantly due to local geology such as uranium content and permeability of underlying rock and soil. The radon gas that leaks from the soil under buildings is the main reason for the spread of this gas in the air inside buildings and work places. As it is emitted from rocks, radon travels to the soil, and attenuates its concentration in the air before seeping into buildings. Granite rocks, metamorphic igneous rocks, clays, and soils contain large amounts of uranium and radium, which are converted to radon through the decay process.

Indoor radioactive radon gas concentration depends on local geology and the rate at which air enters and exits including the design of the house, the ventilation habits of the residents, and the tightness of the air inlets in the building. Radon gas enters homes through cracks in floors or where floors meet walls, gaps around pipes or cables, or small holes in walls made of vacuum moldings, sinks, or sewers. Radon concentrations are usually higher in basements, and living spaces in contact with the soil, but radon can also be found in high concentrations above the ground floor.

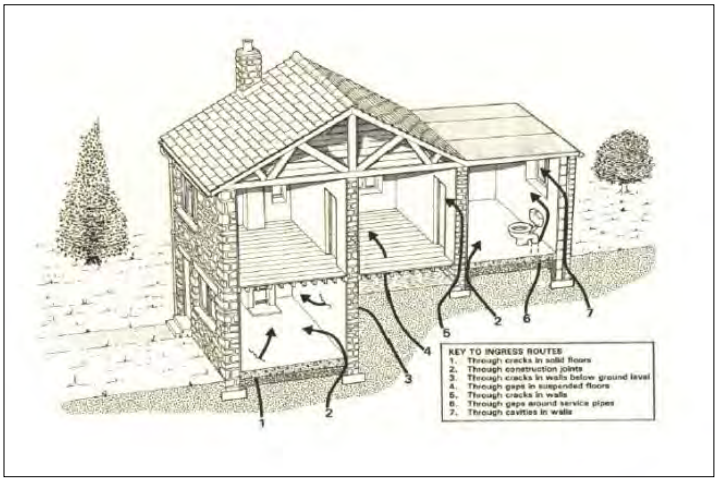

Fig 2: Shows how radon enters homes. [6]

3.1- Reduction of radon concentration indoors:

There are well-proven, sustainable and cost-effective methods for preventing radon risks in new homes and workplaces and reducing radon concentrations in existing dwellings. Radon protection should be considered when constructing new buildings, particularly in radon-prone areas. In many countries in Europe, the USA and China, measures to protect against radon in new buildings are included in building codes.

Outdoors, radon evaporates quickly, concentrations are minimal, and it is generally not a problem. The average outdoor radon concentration ranges between 5 and 15 Bq/m3. Conversely, radon concentrations are higher in enclosed spaces and poorly ventilated areas, with the highest levels recorded in places such as mines, caves, and water treatment facilities. Radon concentrations in buildings such as homes, schools and offices can vary greatly from 10 Bq/m3 to more than 10,000 Bq/m3. Given

the characteristics of radon, residents of such buildings may live or work in them not knowing that the radon concentration levels are extremely high. To reduce radon levels in existing buildings, ventilation below the floor must be increased. Installing a radon collection system in the basement or under a solid floor; preventing radon leakage from basements into living rooms; In addition to sealing floors and walls and finally, improving the ventilation of the building, especially in the context of energy conservation. Passive mitigation systems have been shown to reduce indoor radon concentrations by more than 50%. If radon exhaust fans are used, these concentrations can be reduced to much less.

3.2- Radon Mitigation Systems:

Radon mitigation is a process or a system used to reduce the indoor radon concentration level as low as possible in buildings. Figure 3 presents the mitigation systems that is used for the reduction of the radioactive radon gas level in buildings. Radon mitigation systems in buildings use a simple technique. This technique consists of a fan to continually draw air from the soil and vent it outdoors using a tube extending to the edge of the roof. This tube can pass either inside or outside the house and vents outside, away from windows and vents. In addition, sealing cracks and openings in the foundation help limiting the flow of the radioactive radon gas and makes the radon mitigation system more efficient. These systems should reduce radon below the EPA action level.

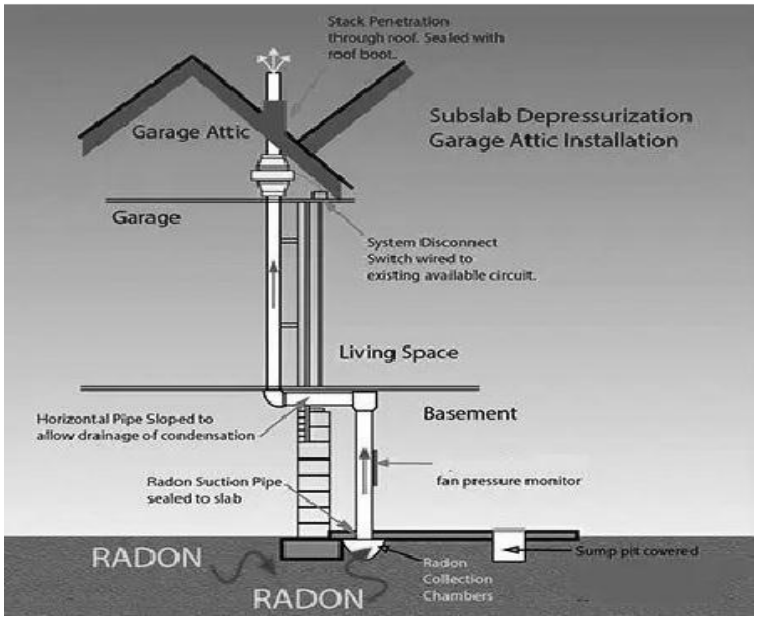

Fig 3: The Mitigation System [7]

4- Radon Sources:

The main sources of radon are soil, rocks, water, and building materials. Studying radon in these

sources is a long process, but in this research we will briefly present these sources.

4.1- Radon in water:

Radon is moderately soluble in water, and its solubility increases with the decrease in water temperature. Therefore, when the cold groundwater runs through the rocks, it absorbs some of the radon gas. Radon can decompose and accumulate in groundwater, as in the case of water pumps or wells drilled in geological regions rich in uranium. Many countries obtain

drinking water from groundwater sources such as springs, surface wells, and artesian wells. These water sources usually contain higher concentrations of radioactive radon than surface water from reservoirs, rivers or lakes. Radon in water can be released into the air when the water is used routinely, such as for showering or washing. No relation have been yet confirmed between the consumption of drinking water containing radon and an increased risk of stomach cancer. Radon gas dissolved in drinking water can escape into the indoor air of buildings.. It is well known that the health risks resulting from drinking water containing radon are very small. The danger mostly results from inhaling radon in the air from the water [8]. The inhaled dose of radon is usually higher than the ingested dose. When the radon is released from the water, it will then diffuse throughout the house before escaping to the outside. In order to raise the whole house average radon levels by 1 pCi/l in a house it is estimated that you need $10{,}000$ pCi/l in the water. This is a general rule that varies according to the size of the house, number of residents, and water usage. Using this ratio requires $40{,}000$ pCi/L in the water in order to raise the average radon levels by 4.0 pCi/L. However, 4.0 pCi/L is not a safe level but a readily achievable level. Since radon in water levels approach or exceed $20{,}000$ pCi/l serious consideration should be given to having a water treat system installed. In order to reduce the indoor levels of radon to 1 pCi/L, we should reduce radon in water levels of $10{,}000$ pCi/L. This will reduce the lifetime of cancer risk of 5 individuals per 1000 persons in the general population. Experiments have shown that the proportion of radioactive isotopes of radium or radon in water can be reduced to internationally permitted levels in simple and inexpensive ways, such as various aeration methods to expel radioactive gases. Some of them may require chemical

water treatments at the source and inside the purification plants and before they reach use or the human body.

4.2- Radon in Soil and Rocks:

About 80% of the radon gas emitted in the outer medium is produced by the upper layer of the earth, and the presence of radium-222 and uranium-232 is the reason for the release of radon gas in the soil. The amount of radium and uranium varies from place to place depending on the geological nature. In general, the rocks in the earth's crust contain about 1 milliCurie per gram, and the soil contains about 4.4 milliCurie per gram. Each disintegration of a radium atom present in soil and rock grains will yield a radon atom. If the production of this atom is close to the surface of the soil, in this case it can leak into the outer medium. Studies have shown that about 10% of the radon generated per meter closest to the earth's surface is released to the outside environment.

Soil is the main source of radon gas in indoor and outdoor air, where radon concentrations are very high up to tens of Bq/m3. The leakage of radon gas from the soil into the atmosphere depends on the concentration of radium (^{226}Ra), Soil properties such as porosity, density, moisture as well as weather factors such as air temperature, pressure, wind and precipitation. Outdoor radon concentrations are relatively low and change daily and seasonally. These changes may be used to study the movement of air masses and other climatic conditions [9]. Radioactive radon gas enters buildings and workplaces through cracks and leaks that occur in the foundations and connections between different materials in the building.

4.3- Radon in building materials:

Building materials made of soil and rocks such as cement, bricks and ceramics contain radioactive materials of natural origin such as uranium and radium and thus generate radon. These materials are permeable enough for the radon generated within them to be released to the outside environment. Many homes contain decorative rocks and stones, such as granite and marble. Because these rocks were formed in the Earth's crust, they may include a small amount of naturally-occurring radioactive materials from Earth such as radon gas. By studying some other materials, it was found that ceramics and cement are among the materials that emit a high percentage of radon gas.

5- Health effects of radon gas exposure:

Radioactive radon gas is a major cause of lung cancer. It is estimated that radon causes between 3% to 14% of all lung cancers in a country, depending on the national average radon level and the smoking prevalence. An increased rate of lung cancer was first seen in uranium miners exposed to very high concentrations of radon [10]. In addition, studies in Europe, North America and China have confirmed that even low concentrations of radon such as those commonly found in residential settings, also pose health risks and contribute to the occurrence of lung cancers worldwide. The risk of lung cancer increases by about 16% per 100 Bq/m3 increase in long time average radon concentration. The dose-response relation is assumed to be linear – i.e. the risk of lung cancer increases proportionally with increasing radon exposure.

Radon is much more likely to cause lung cancer in people who smoke. In fact, smokers are estimated to be 25 times more at risk from radon than non-smokers. No other cancer risks or other health effects have been established to date, although inhaled radon can deliver radiation to other organs, but at a much lower level than to the lungs. Its danger depends on the amount and percentage of its concentration in the air surrounding the person, and also on the time period in which the person is exposed to it.

The health effects of radon lie in the alpha particles it emits and its breakdown products. Where these particles have enough energy to penetrate the tissues and reach the inner part of the cells and destroy these tissues. There are two ways that radon and its breakdown products can enter the human body: breathing and digestion. It is believed that digestion is not dangerous, as the presence of food in the stomach, even with a thickness not exceeding 1.5 mm, can stop most of the alpha particles issued by the disintegration of radon and its offspring. Since radon is a noble gas with a large half-life compared to the respiratory cycle, it either passes into the circulatory system or returns and is exhaled from the lung. And since the radon disintegration products attach themselves to air suspensions, they have a high probability of entering the lung, disintegrating and harming the lung.

It has been estimated that around 6% of lung cancer cases in the UK can be attributed to radon. It was also mentioned in the fourth report of the committee composed for the study of the biological effect of ionizing radiation that about 10% of cancerous injuries are the result of radon gas. In their report, they hypothesized that the risk interaction between radon and smoking is a multiplicative rather than an additive relationship. This

hypothesis was found to be consistent with information collected on miners in Colorado and Mexico. Some studies also showed that some types of cancer such as leukemia, kidney cancer, and protozoa can be attributed to exposure to radon gas.

All of the aforementioned is based on the results obtained from the exposure of miners to radon gas during their work periods, except that the situation in buildings is different. The air inside the mine is very dusty, which increases the suspension of radon disintegration products and changes the balance coefficient. The breathing of workers during their work is deep compared to that at home, which increases the amount of air entering the lung. All of this makes the use of miners' findings in estimating household radon exposure questionable.

6- Protection against risk of radon exposure:

With regard to radon gas in water, experiments have shown that the proportion of radioactive isotopes of radium or radon in water can be reduced to internationally permitted levels by simple and inexpensive methods such as various ventilation methods to expel radioactive gases. Some of them may require chemical water treatments from the source and inside Purification plants before they reach use or the human body. The permissible limits according to US and other international standards for radium levels in drinking water should not exceed 5 pCi/l, while the permissible limits for radon gas levels according to American specifications should not exceed 300 pCi/l.

As for the indoor radon, it can be disposed off through the process of ventilation when opening doors and windows and not living in the lower

floors to avoid radon rising from the ground. Although the dissolution of radium found in building materials and granite is not fast, the permanent ventilation of homes will make its presence almost non-existent. Also, the soil content of radioactive substances and the rate of radon gas flow from it must be known before carrying out construction operations. If it is high, the surface crust of the soil must be removed. It also raises the floor level of the building to a high level relative to the surface of the ground, and this allows the movement of air under the building, which leads to a reduction in the rate of radon leakage inside the building. One other way of protection against radon is to spend less time in places with high concentrations of this deadly gas and opening windows and operating fans to increase air flow in buildings. Properly closing and covering manholes limits radon leakage into buildings and homes. In addition to measuring the rates of radon decomposition products using multiple detectors and the need to inform the competent authorities if the measured value exceeds the limits mentioned in WHO.

8- Summary:

In the present, an overview of the radioactive gas radon and its sources have been presented to draw attention to the health effects of this radioactive gas and the ways of how people can protect themselves from its deadly risks.

8- References:

[1] MADDEN, J. S, "Personal monitoring of tour guides in Irish show caves", Protection Against Radon at Home and at Work (Proc. Eur. Conf. Prague, 1997), Part II, FJFI VUT, Prague (1997) 123-128.

[2] **Lubin JH**, **Boice JD Jr**. "Lung cancer risk from residential radon: meta-analysis of eight epidemiologic studies " Journal of the National Vancer Institute, Vol. 89, No. 1, Jan. 1997.

[3] E. Dorn, Über die von radioaktiven substanzen ausgesandte emanation. Abhandlungen derNaturforschenden Gesellschaft zu Halle (Stuttgart) 22, 155, (1900).

[4] Fatema S. Abd Ali, et al."Humidity effect on diffusion and length coefficient of radon in soil and building materials" Science direct, Energy Procedia 157(2019) 384-392.

[5] UNSCEAR (United Nations Scientific Committee on the Effects of Atomic Radiation), "Effects and Risks of Ionizing Radiations," United Nations, New York, 2000.

[6]C. H. CLEMENT, Radiological Protection against Radon Exposure, Annuals of the ICPR, Elsevier, ICRP ref 4829-9671-655. 2011 December 6 2.

[7] Wikipedia the free encyclopedia

[8] Bill Brodhead, WPB Enterprises Inc, Radon & Vapor Intrusion, Consultant - Researcher – Instructor, Website Information Provider.

[9] Maize and development, Arab Atomic Energy Authority. vol 19, 4 (2007).

[10] Radiation risks between the environment and legislation in the Arab world/ Mamdouh Hamid Attia, Sahar Mustafa Hafez - Dar Al-Fikr Al-Arabi, 2005.

Journal of Total Science
Volume (6), Issue (23) March. 2023)
ISSN: 2518-5799

مجلة العلوم الشاملة
المجلد (6)، العدد (23)، (مارس2023)
ردمد: 2518-5799

Resulting potential for interior region and exteriorregion of a spherical shall in spherical coordinate

Hana JummaAljerbi
Nalut University , Faculty of medical technology
Collegeofmedicaltechnologynalut.blogspot.com

ABSTRACT :

In this work, I have presented potential interior region and exterior region of the sphere using sphericalcoordinate, azimuthal symmetry ,and separation of variables then I get the general solution of potential:

$v(r , \theta) = \sum_{l=0}^{\infty} (A_l r^l + \frac{B_l}{r^{l+1}}) p_l (\cos\theta)$.

The interesting feature of this solution is linear combination of separable solution. Furthermore, this solution I do it to solve the problem that need to calculate thepotential in any region where there is no charge;$v_0(\theta)$ is specified on the surface of a sphere inside ($r \leq R$) and outside($r \geq R$) the sphere. Finally, I show that we can find the potential inside and outside spherical shell of radius R , and specified charge density $\sigma_0(\theta)$ is glued over the surface of this spherical shall.

KEY WORDS:AZIMUTHAL SYMMETRY- LEGENDRE POLYNMIALS- BOUNDRU CONDITION- RODRIGUES FORMULA

Introduction

I want to determine the potential inside the sphere,r <R, outside the sphere, r > R, and of course I would also like to know what happens at r = R. So the regionwhere I want to determine the potential is"everywhere", or all space. To pose a problem with aunique solution I need to describe any charge inside this region, and also specify the potential on theboundary of the region. In spherical coordinates the Laplace equation takes the form :

$$\frac{1}{r^2}\frac{\partial}{\partial r}\left(r^2\frac{\partial V}{\partial r}\right)+\frac{1}{r^2 sin\theta}\frac{\partial}{\partial \theta}\left(\sin\theta\frac{\partial V}{\partial \theta}\right)+\frac{1}{r^2 sin^2\theta}\frac{\partial^2 V}{\partial \phi^2}=0. \qquad (1.1)$$

I shall assume the problem has **azimuthal symmetry**, so that V is independent of ϕ, in that case Eq. 1.1 reduces to

$$\frac{\partial}{\partial r}\left(r^2\frac{\partial V}{\partial r}\right)+\frac{1}{sin\theta}\frac{\partial}{\partial \theta}\left(\sin\theta\frac{\partial V}{\partial \theta}\right)=0\ . \qquad (1.2)$$

Spherical coordinate

Now I look for solution that are products :

$$V(r,\theta)=R(r)\Theta(\theta)\ . \qquad (1.3)$$

Putting this into Eq. (1.2) and dividing by V :

$$\frac{1}{R}\frac{\partial}{\partial r}\left(r^2\frac{\partial R}{\partial r}\right)+\frac{1}{\Theta\, sin\theta}\frac{\partial}{\partial \theta}\left(\sin\theta\frac{\partial \Theta}{\partial \theta}\right)=0\ . \qquad (1.4)$$

Since the first term depends only on r , and the second only on θ, it follows that each must be a constant:

$$\frac{1}{R}\frac{\partial}{\partial r}\left(r^2\frac{\partial R}{\partial r}\right)=\boldsymbol{l}(\boldsymbol{l}+1)\ ,\quad \frac{1}{\Theta\, sin\theta}\frac{\partial}{\partial \theta}\left(\sin\theta\frac{\partial \Theta}{\partial \theta}\right)=-\boldsymbol{l}(\boldsymbol{l}+1)\boldsymbol{l}. \qquad (1.5)$$

Here $\boldsymbol{l}(\boldsymbol{l}+1)$ is just fancy way of writing the separation constant – you will see in minute why this is convenient.

As always, separation of variables has converted a partial differential equation(1.2) into ordinary differential equations (1.5). The radial equation ,

$$\frac{\partial}{\partial r}\left(r^2\frac{\partial R}{\partial r}\right)=\boldsymbol{l}(\boldsymbol{l}+1)\,R, \qquad (1.6)$$

has the general solution

$$R(r)=Ar^{l}+\frac{B}{r^{l+1}}\ , \qquad (1.7)$$

A and B are the two arbitrart constant to be expected in the solution of a second –order differential equation. But the angular equation,

$$\frac{\partial}{\partial \theta}\left(\sin\theta\frac{\partial \Theta}{\partial \theta}\right)=-\boldsymbol{l}(\boldsymbol{l}+1)\boldsymbol{l}\sin\theta\Theta, \qquad (1.8)$$

Is not so simple . The solution are **Legendre polynomials** in the variable cosθ : $\Theta(\theta) = p_l(\cos\theta)$. (1.9)

$p_l(x)$ is most conveniently defined by **Rodrigues formula** :

$p_l(x) = \frac{1}{2^l\, l!}(\frac{d}{dx})^l\ (x^2 - 1)^l$. (1.10)

Note that $p_l(x)$ is an $\boldsymbol{l}$th-order polynomial in x; it contains only even powers, if $\boldsymbol{l}$ is even, and odd powers, if $\boldsymbol{l}$ is odd. The factor in front $(\frac{1}{2^l\, l!})$ was chosen in order that $p_l(1) = 1$. (1.11)

The Rodrigues formula obviously works only for nun negative integer values of $\boldsymbol{l}$. Moreover, it provides us with only one solution . But Eq. (1.8) is second-order, and it should possess tow independent solution, for every value of $\boldsymbol{l}$. It turns out that these "other solution" blow up at θ=0 and/or θ=π, and therefore unacceptable on physical grounds. [1] For instance, the second solution for $\boldsymbol{l} = 0$ is

$\Theta(\theta) = \text{Ln}\ (\tan\frac{\theta}{2})$. (1.12)

In case of azimuthal symmetry, then, the most general separable solution to Laplace's equation, consistent with minimal physical requirements, is

$V(r,\theta) = (A_l r^l + \frac{B_l}{r^{l+1}})\ p_l(\cos\theta)$.

(There was no need to include an overall constants in Eq. (1.9) because it can be absorbed into A and B at this stage.) Separation of variables yields an infinite set of solutions, one for each $\boldsymbol{l}$. The general solution is the linear combination of separation solutions:

$v(r\ ,\ \theta) = \sum_{l=0}^{\infty}\ (A_l r^l + \frac{B_l}{r^{l+1}})p_l\ (\cos\theta)$. (1.13)

This result is so important, as well as I make it in the simple formula to solve all problems of potential in spherical shall. The following problems illustrate the power of this important result.

PROBLEM 1

The potential $V_0(\theta)$ is specified on the surface of a hollow sphere, of radius R. Find the potential inside the sphere ?

Solution : In this case $B_l = 0$ for all l –otherwise the potential blow up at origin. Thus, $v(r,\theta) = \sum_{l=0}^{\infty} (A_l r^l) p_l(\cos\theta)$. (1.14)

At r = R this must match the specified function $V_0(\theta)$:

$V(R,\theta) = \sum_{l=0}^{\infty} (A_l R^l) p_l(\cos\theta) = V_0(\theta)$. (1.15)

Can this equation be satisfied, for an appropriate choice of coefficients A_l ?

Yes: The legendary polynomials (like the sins) constitute a complete set of functions, on the interval $(-1 \le x \le 1)$, $(0 \le \theta \le \pi)$. Now determine the constants by Fourier's trick, for the Legendre polynomials are orthogonal functions:

$$\int_{-1}^{1} p_{l(x)}\, p_{l'(x)} dx = \int_0^{\pi} p_{l(\cos\theta)}\, p_{l'(\cos\theta)} \sin\theta\, d\theta$$

$$= \begin{cases} 0, & if\ l' \neq l \\ \frac{2}{2l+1}, & if\ l' \neq l \end{cases} \quad (1.16)$$

Thus multiplying Eq.(1.15) by $p_{l'}(\cos\theta)\sin\theta$ and integrating, we have

$$A_l R^l \frac{2}{2l+1} = \int_0^{\pi} V0\,(\theta)\, p_{l'}\,(\cos\theta)\, \sin\theta\, d\theta.$$

$$A_l = \frac{2l+1}{2R^l} \int_0^{\pi} V0\,(\theta)\, p_{l'}\,(\cos\theta)\, \sin\theta\, d\theta. \quad (1.17)$$

Equation (1.14) is the solution of our problem, with the coefficients given by Eq.(1.17). It can be difficult to evaluate the form (1.17) analytically, and in practice it is often easier to solve Eq.(1.15) "by eyeball."For instance, suppose we are told that the potential on the sphere is

$$V_0(\theta) = k \sin^2(\theta/2), \quad (1.18)$$

Where k a constant . Using the half–angle formula, we rewrite this as

$$V_0(\theta) = \frac{k}{2}(1 - \cos\theta) = \frac{k}{2}\left(p_0(\cos\theta) - p_1(\cos\theta)\right).$$

Butting this into Eq.(1.15), we read of immediately that $A_0 = k/2$, $A_1 = -k/(2R)$, and all other A_l s' vanish. Evidently,

$$V(r,\theta) = \frac{k}{2}\left(r^0 P_0(\cos\theta) - \frac{r^l}{R} P_1(\cos\theta)\right) = \frac{k}{2}\left(1-\frac{r}{R}\cos\theta\right). \qquad (1.19)$$

PROBLEM 2

The potential $V_0(\theta)$ is specified on the surface of a hollow sphere, of radius R. But this time we asked to Find the potential outside the sphere, assuming there is no charge there ?

Solution : in this case the $A_l$must be zero (or else V would not go to zero at ∞), so

$$v(r,\theta) = \sum_{l=0}^{\infty} \left(\frac{B_l}{r^{l+1}}\right) p_l(\cos\theta). \qquad (1.20)$$

At the surface of the sphere we required that

$$v(R,\theta) = \sum_{l=0}^{\infty} \left(\frac{B_l}{R^{l+1}}\right) p_l(\cos\theta) = V_0(\theta).$$

Multiplying by $p_{l'}(cos\theta)\, sin\theta$ and integrating – exploiting, again, orthogonality relation (1.16) we have

$$\frac{B_l}{R^{l+1}}\frac{2}{2l+1} = \int_0^{\pi} V0(\theta)\, p_{l'}(cos\theta)\, sin\theta\, d\theta ,$$

$$B_l = \frac{2l+1}{2} R^{l+1} \int_0^{\pi} V0(\theta)\, p_{l'}(cos\theta)\, sin\theta\, d\theta. \qquad (1.21)$$

Equation (1.20),with the coefficients given by Eq.(1.21) is the solution of our problem.

PROBLEM 3

An un charged metal sphere of radius R is placed in an otherwise uniform electric field $E=E_0\hat{z}$. (The field will push positive charge to the "northern" surface of sphere, leaving a negative charge on the "southern" surface.

This induced charge in turn, distorts the field in the neighborhood of the sphere. Find the potential in the region outside the sphere ?

Solution : The sphere is an equipotential –we may as well set it to zero. Then by symmetry the entire (x y) plane is at potential zero. This time, however, V does not go to zero at large z. In fact, far from the sphere the field is $E_0\hat{z}$, and hence

$$V \to -E_0 z + C .$$

Since V=0 in the equatorial plane, the constant C must be zero. Accordingly, the boundary condition for this problem are

1 – V=0 when r = R.(1.22)

2 – $V \to -E_0 r\cos\theta$ for $r \gg R$. (1.22)

We must fit these boundary conditions with a function of the form (1.13). The first condition yields

$$A_l r^l + \frac{B_l}{r^{l+1}} = 0 .$$

Or $B_l = -A_l R^{2l+1}$,

So $v(r,\theta) = \sum_{l=0}^{\infty} A_l\left(r^l - \frac{R^{2l+1}}{r^{l+1}}\right)p_l(\cos\theta)$. (1.23)

for $r \gg R$, the second term in parentheses isnegligible, and therefore condition (2) requires that

$$\sum_{l=0}^{\infty} (A_l R^l)p_l(\cos\theta) = -E_0 r\cos\theta .$$

Evidently, only one term is present: $l = 1$. In fact, since $p_1(\cos\theta) = \cos\theta$, we can read off immediately

$E_1 = -E_0$, all other A_l = zero.

Conclusion:

$V(r,\theta) = -E_0 \left(r - \frac{R^3}{r^2}\right)\cos\theta.$ (1.24)

The first term $(-E_0\ r\cos\theta)$ is due to the external field; the contribution attributable to the induced charge is evidently

$E_0 \left(r - \frac{R^3}{r^2}\right)\cos\theta$.

The induced charge density, it can be calculated by

$\sigma(\theta) = -\epsilon_0 \frac{\partial V}{\partial r}\Big|_{r=R} = \epsilon_0 E_0 \left(r - 2\frac{R^3}{r^3}\right) cos\theta \Big|_{r=R} = 3\epsilon_0 E_0 Cos\theta.$

As expected it is positive in the northern hemisphere ($0 \le \theta \le \pi/2$) and negative in southern $(\pi/2 \le \theta \le \pi)$.

==========

Conclusion :

In this work I present a solution of potential in the case of azimuthal symmetry, the most general separable solution to Laplace's equation consistent with minimal physical requirements:

$v(r,\theta) = \left(Ar^l + \frac{B^l}{r^{l+l}}\right) P_l(\cos\theta).$

The A_l and B_l are constants, and the $P_l(\cos\theta)$ are Legendre polynomials. The coefficients A_l andB_l tell us how much of each separable solution { r^l $P_l(\cos\theta)$ and $(1 / (r^l+1))$ $P_l(\cos\theta)$.}to include toget the actual potential we want.

Where; the first part of that equation considered the potential inside a sphere, and the second part considered the outside potential of sphere.

we also have access to powerful techniques that help with problems where there is much less symmetry.Separation of variables can be used to build up solutions to problems that depend on r, θ, and$\emptyset$.

==========

REFERENCES

1. M. A. Heald's J. B. Marion's classical 3rd(third)edition classical electromagnetic radiation (Hardcover) 1994.
2. J. D. Jackson classical Electrodynamics 3rd third edition ISBN-13:978047130921,ISBN-10 .
3. M. L. Boas Mathematical Methods in PhysicalSciences 3rd third edition . ISBN 13:9780471198260,ISBN10:9780471198260
4. M. Akbar and R.-G. Cai, Thermodynamic behavior of Friedmann equations at apparent horizon of FRW universe, Phys. Rev. D 75 (2007) 084003 [hep-th/0609128] [INSPIRE].
5. A.M. Awad and C.V. Johnson, Holographic stress tensors for Kerr-AdS black holes, Phys. Rev. D 61 (2000) 084025 [hep-th/9910040] [INSPIRE].
6. A.M. Awad and C.V. Johnson, Scale versus conformal invariance in the AdS/CFT
7. correspondence, Phys. Rev. D 62 (2000) 125010 [hep-th/0006037] [INSPIRE].
8. 7 G.G.L. Nashed, A special exact spherically symmetric solution in f(T) gravity theories,Gen. Rel. Grav. 45 (2013) 1887 [arXiv:1502.05219] [INSPIRE].
9. D. J. Griffiths , Introduction to Electrodynamics ISBN:81-7758-293-3
10. M. Baum, M.A.J. Chaplain, A.R.A. Anderson, M. Douek, J.S. Vaidya, Eur. J. Cancer 35 (1999) 886.

11. M. Itik, S.P. Banks, Int. J. Bifurcation Chaos 20 (2010) 71.
12. G. Contopoulos, N. Voglis (Eds.), Galaxies and Chaos, Springer, 2003.
13. G. Contopoulos, Order and Chaos in Dynamical Astronomy, Springer, 2004.
14. R.C. Hilborn, Chaos and Nonlinear Dynamics, An Introduction for Scientists and Engineers, second ed., Oxford
15. University Press, 2001.
16. Y.A. Kuznetsov, Elements of Applied Bifurcation Theory, second ed., Springer-Verlag, 1998.
17. MinghuiXu, D.A. Tieri, E.C. Fine, James K. Thompson, M.J. Holland, Phys. Rev. Lett. 113 (2014) 154101.
18. J.M. Weiner, K.C. Cox, J.G. Bohnet, J.K. Thompson, Phys. Rev. A 95 (2017) 033808.
19. A. Patra, B.L. Altshuler, E.A. Yuzbashyan, Phys. Rev. A 99 (2019) 033802.
20. A. Patra, B.L. Altshuler, E.A. Yuzbashyan, Phys. Rev. A 100 (2019) 023418.
21. H. Goldstein, C. Poole, J. Safko, Classical Mechanics, Addison Wesley, 2000.
22. A. Uchida, Optical Communication with Chaotic Lasers, Wiley-VCH, 2012.
23. L.M. Pecora, T.L. Carroll, G.A. Johnson, D.G. Mar, Chaos 7 (1997) 520.
24. L.M. Pecora, T.L. Carroll, Phys. Rev. Lett. 64 (1990) 821.
25. S. Hayes, C. Grebogi, E. Ott, A. Mark, Phys. Rev. Lett. 73 (1994) 1781.

26. P.M. Alsing, A. Gavrielides, V. Kovanis, R. Roy, K.S. Thornburg Jr., Phys. Rev. E 56 (1997) 6302.
27. H.G. Winful, L. Rahman, Phys. Rev. Lett. 65 (1990) 1575.
28. R. Roy, K.S. Thornburg Jr., Phys. Rev. Lett. 72 (1994) 2009.
29. T. Fukuyama, R. Kozakov, H. Testrich, C. Wilke, Phys. Rev. Lett. 96 (2006) 024101.
30. B. Blasius, A. Huppert, L. Stone, Nature 399 (1999) 354.
31. M. de Sousa Vieira, Phys. Rev. Lett. 82 (1999) 201.
32. W. Tucker, Physica D 171 (2002) 127.
33. H.J. Carmichael, Statistical Methods in Quantum Optics 1 – Master Equations and Fokker–Planck Equations,
34. Springer–Verlag Berlin Heidelberg, 1999.
35. H.J. Carmichael, Statistical Methods in Quantum Optics 2 – Non–Classical Fields, Springer–Verlag, 2008.
36. H.J. Carmichael, An Open System Approach To Quantum Optics, Springer–Verlag Berlin Heidelberg, 1993.
37. [26] R. Bonifacio, P. Schwendimann, Fritz Haake, Phys. Rev. A 4 (1971) 302.
38. [27] A.D. Ludlow, M.M. Boyd, T. Zelevinsky, S.M. Foreman, S. Blatt, M. Notcutt, T. Ido, J. Ye, Phys. Rev. Lett. 96 (2006)
39. 033003.
40. [28] D. Meiser, Jun Ye, D.R. Carlson, M.J. Holland, Phys. Rev. Lett. 102 (2006) 163601.
41. [29] Here the TSS (one fixed point) gives rise to the NTSS, which is a collection of fixed points lying on a circle
Blackwood, O H, Kelly, W C, and Bell, R M, General Physics, 4th Edition, Wiley, 1973

42. Craford, M. George, Holonyak, Nick, and Kish, Frederick, "In Pursuit of the Ultimate Lamp", Scientific American 284, 62, February 2001.
43. Denardo, Bruce, Temperature of a Lightbulb Filament, The Physics Teacher 40, 101, February 2002.
44. Diefenderfer, James and Holton, Brian, Principles of Electronic Instrumentation, 3rd Ed. ,Saunders College Publ., 1994.
45. Diefenderfer, James, Principles of Electronic Instrumentation, 2nd Ed. , W.B. Saunders, 1979.
46. Giancoli, Douglas C., Physics, 4th Ed, Prentice Hall, (1995).
47. Ewell, George W., Radar Transmitters, McGraw-Hill, 1981.
48. Floyd, Thomas L., Electric Circuit Fundamentals, 2nd Ed., Merrill, 1991
49. Floyd, Thomas L., Electronic Devices 3rd Ed., Merrill, 1992
50. Halliday&Resnick, Fundamentals of Physics, 3E, Wiley 1988
51. Halliday, Resnick& Walker, Fundamentals of Physics, 4th Ed, Extended, Wiley 1993
52. Horowitz, Paul and Hill, Winfred,The Art of Electronics, Cambridge University Press, 1980
53. Jackson, J. D., Classical Electrodynamics, Wiley (1975).
54. Jones, Edwin R (Rudy) and Childers, Richard L, Contemporary College Physics, Addison-Wesley, 1990. A well-illustrated non-calculus introductory physics text.
55. Jung, Walter, IC Op-Amp Cookbook, Howard Sams, 1981
56. Kip, Arthur F., "Fundamentals of Electricity and Magnetism, 2nd Ed.", McGraw-Hill, 1969.
57. Kittel, Charles, "Introduction to Solid State Physics, 2nd Ed.", Wiley, 1956.

58. Ladbury, Ray, "Geodynamo Turns Toward a Stable Magnetic Field", Physics Today 49, Jan 96, pg 17.
59. Mims, Forrest M, Op Amp IC Circuits, Engineer's Mini-Notebook, Cat. No. 276-5011A, Radio Shack 1985
60. Mims, Forrest M, Digital Logic Circuits, Radio Shack 1985
61. Mims, Forrest M., Getting Started in Electronics, Radio Shack, 1983
62. Mims, Forrest M., 555 Timer IC Circuits, 3rd Ed, Engineer's Mini-Notebook, Radio Shack Cat. No. 276-5010A, 1992
63. Mims, Forrest, Optoelectronic Circuits: Engineers Mini-Notebook, Radio Shack Cat. No. 276-5012, 1986. Small notebook with practical details and sketches of circuit applications.
64. Nave & Nave, Physics For the Health Sciences, 3rd Ed, W. B. Saunders, 1985
65. Ohanian, Hans, Physics, 2nd Ed. Expanded, Norton, 1985.
66. Reitz, J., Milford, F. and Christy, R., Foundations of Electromagnetic Theory, 4th Ed, Addisonpitchfork bifurcation. They correspond to $\Phi = \Phi 0$ and $\pi + \Phi 0$.

Journal of Total Science
Volume (6), Issue (23) March. 2023)
ISSN: 2518-5799

مجلة العلوم الشاملة
المجلد (6)، العدد (23)، (مارس2023)
ردمد: 2518-5799

Analysis of a three-Phase Induction Motor with Open Stator Phase Using an Equivalent Two-Phase Model

تحليل محرك تحريضي ثلاثي الأطوار مع طور ساكن مفتوح باستخدام نموذج مكافئ ثنائي الطور

Said Ahmed
سعيد احمد
Higher insitute of science and Tchnology. Regdalin .
Libya
المعهد العالي للعلوم والتقنية. رقدالين. ليبيا

Fouad Eltoumi
فؤاد التومي
Libyan authority for scintific research. Tripoli.
Libya
طرابلس. ليبيا.الهيئة الليبية للبحث العلمي

الملخص :

يقدم هذا البحث نمذجة لمحرك تيار متردد ثلاثي الأطوار الذي يحتوي على مرحلة ستاتور مفتوحة. يتمحور التركيز في البحث حول دراسة الاستجابة الديناميكية للمحرك في مختلف السيناريوهات التشغيلية، سواء كانت عادية أو معطوبة. يستخدم البحث نموذجاً ثنائي الأبعاد d-q يشير إلى الإطار المرجعي الثابت، مما يسمح بتحليل دقيق ومحكم لسلوك المحرك. يستخدم برنامج Matlab لإجراء المحاكاة وتحليل البيانات. من خلال هذه المحاكاة، يتم دراسة أداء المحرك تحت مختلف الظروف التشغيلية، بما في ذلك التغييرات في الحمل والجهد والتردد. كما يتم دراسة استجابة المحرك لأنواع مختلفة من الأخطاء، مثل قضبان الدوران المكسورة أو أخطاء لف المرحلة. تشرح النتائج فعالية طريقة النمذجة المقترحة في تحليل السلوك الديناميكي لمحرك التيار المتردد ثلاثي الأطوار المفتوح المرحلة. من خلال استخدام نموذج الأبعاد d-q ذو الاثنين من المراحل، يتم الحصول على فهم أعمق لسلوك المحرك وخصائص أدائه في ظروف التشغيل المختلفة. تمتلك نتائج هذا البحث نتائج هامة لتصميم وتحسين أنظمة محركات التيار المتردد ويمكن أن تساهم في تعزيز موثوقيتها وكفاءتها في مختلف التطبيقات الصناعية والتجارية

1. Introduction

Induction motors (IMs) are commonly utilized across different industrial applications, thanks to superior efficiency and robust performance with minimal maintenance needs. Despite their reliability, IMs are susceptible to different types of faults, which can significantly affect their performance.

One of the most common faults in IMs is the open circuit of a stator winding.When one phase of an induction motor is open circuited, once a phase is lost in the motor, there is no longer any mutual coupling interaction between the lost phase and the remaining phases, leading to a drastic change in the dynamic behavior of the motor[1, 2]. Therefore, an accurate and precise modeling approach is essential for analyzing the dynamic behavior of an induction motor with an open stator phase. When modeling induction motors, the most commonly used approach is the two-dimensional d-q model or 2-phasemodel. Nonetheless, the unbalanced configuration of a 3-phase motor with Isolated phase means that the 2-phase d-q model of a normal motor differs from that of a faulty one. Therefore, an accurate and precise modeling approach is essential for analyzing the dynamic behavior of an induction motor with an open stator phase.

Several studies have investigated the dynamic behavior of induction motors with open stator phases using different modeling techniques. For instance, S. Limayein [1] have proposed a 3-phase IM model with an open stator phase using the Park transformation technique. The authors demonstrated that the proposed model accurately captures the dynamic operation of the motor under various operating circumstances. Similarly, K. S. Sandhu [2] investigated the effect of an open stator phase on the performance of an IM using a two-phase model. The authors demonstrated that the proposed model accurately predicts the motor's behavior in various operating conditions. In another study, Chitti Babu et al. [3] have proposed a fuzzy-neural network-based approach for detecting open stator faults in induction motors. The authors demonstrated

that the proposed approach achieves high accuracy in detecting open stator faults, which can lead to improved motor performance and reduced maintenance costs.A review of the literature shows that various methods have been used for fault diagnosis of induction motors, including current signal analysis, inductance signature analysis, magnetic field analysis, and current Park's vector approach [1, 2, 3, 5, 9]. Additionally, several studies have investigated the effect of open-circuited stator windings on the dynamic behavior of the motor [4, 5, 6]. Simulation software like Matlab has been used extensively to study these effects [1, 7, 8, 10].

This paper proposes approach for modeling a 3-phase induction motor with an open stator phase using an equivalent 2-phase d-q model. The proposed approach investigates the dynamic performance of the motor under normal and faulty scenarios.

The importance of this study lies in its contribution to improving the performance of induction motor systems. The proposed modeling approach provides a more accurate and precise analysis of the motor's behavior in various operation modes, offering a deeper understanding of its performance characteristics. Such an understanding is critical for enhancing the reliability and efficiency of induction motor systems in various industrial and commercial applications. Through simulations using MATLAB software, this study examines the performance of the induction motor under varying conditions, including load, voltage, and frequency changes. Additionally, it investigates the motor's response to different faults conditions, such as broken rotor bars or stator winding faults. The findings of this study can help design and optimize induction motor systems to improve their reliability and efficiency in various industrial and commercial

applications. Therefore, this study's contribution to the field of induction motor modeling and analysis has significant implications for various industries and sectors.

2. Induction MotorMathematical models

2.1 IM Model in the Park Reference Frame

The IMmodelling in the park reference frame is a widely used technique for modeling and analyzing the behavior of induction motors. It is based on transforming the 3-phase stator currents and voltages into two orthogonal components, namely the direct (d) and quadrature (q) components [11,12]. The Park transformation is a mathematical tool that can be used to transform the 3-phase variables into their corresponding d-q components.

In matrix form, equations (1)-(4) present the 3-phase model for an induction motor that comprises both the stator and rotor. These equations, which are referred to as the voltage mode equations, describe the motor by its terminal voltages and currents [13-15].

Voltage equations:

$$\left[v_{s\_abc}\right]=\left[R_s\right]\left[i_{s\_abc}\right]+\frac{d}{dt}\left[\Phi_{s\_abc}\right] \qquad (1)$$

$$\left[v_{r\_abc}\right]=\left[R_r\right]\left[i_{r\_abc}\right]+\frac{d}{dt}\left[\Phi_{r\_abc}\right] \qquad (2)$$

Flux-currents equations:

The flux-current mode equations represent the motor in terms of its fluxes and currents. The equations are as follows:

$$\left[\Phi_{s\_abc}\right]=\left[L_{ss}\right]\left[i_{s\_abc}\right]+\left[L_{sr}\right]\left[i_{r\_abc}\right] \qquad (3)$$

$$\left[\Phi_{r\_abc}\right]=\left[L_{rs}\right]\left[i_{s\_abc}\right]+\left[L_{rr}\right]\left[i_{r\_abc}\right] \qquad (4)$$

$[v_{s\_abc}]$, $[i_{s\_abc}]$ and $[\Phi_{s\_abc}]$, are :voltage, current and stator flux vectors.

Rotor windings: $[v_{r\_abc}]$, $[i_{r\_abc}]$ and $[\Phi_{r\_abc}]$.

The stator resistance matrix $[R_s]$ and rotor resistance matrix $[R_r]$ as:

$$\left[R_s\right]_{3\times3}=r_s\left[I\right]_{3\times3};\quad \left[R_r\right]_{3\times3}=r_r\left[I\right]_{3\times3}$$

The stator and rotor winding inductance matrices are denoted as [Lss] and [Lrr], respectively, in equations (3)-(4), while [Lsr] and [Lrs] matrices represent the common inductances of the stator and rotor. All of these parameters are identified in [2].

$$\left[L_{ss}\right]_{3\times3}=l_{ls}\left[I\right]_{3\times3}+l_{ms}\begin{bmatrix}1 & -0.5 & -0.5\\ -0.5 & 1 & -0.5\\ -0.5 & -0.5 & 1\end{bmatrix} \qquad (5)$$

$$\left[L_{rr}\right]_{3\times3}=l_{lr}\left[I\right]_{3\times3}+l_{ms}\begin{bmatrix}1 & -0.5 & -0.5\\ -0.5 & 1 & -0.5\\ -0.5 & -0.5 & 1\end{bmatrix} \qquad (6)$$

$$\left[L_{sr}\right]_{3\times3}=l_{ms}\begin{bmatrix}\cos(\theta) & \cos\left(\theta+\frac{2\pi}{3}\right) & \cos\left(\theta-\frac{2\pi}{3}\right)\\ \cos\left(\theta-\frac{2\pi}{3}\right) & \cos(\theta) & \cos\left(\theta+\frac{2\pi}{3}\right)\\ \cos\left(\theta+\frac{2\pi}{3}\right) & \cos\left(\theta-\frac{2\pi}{3}\right) & \cos(\theta)\end{bmatrix} \qquad (7)$$

$$\left[L_{rs}\right]_{3\times3}=\left[L_{sr}\right]^T$$

In equations (5)-(7)[2]:

l_{ls}, l_{ms}:stator leakage and magnetizing inductance.

l_{lr}:the rotor leakage inductance.

θ: rotor angular position.

As illustrated in Fig.1, the IM 2-phase model is defined by park's transformation. Where:

d: direct axis, **q**: quadratic axis.

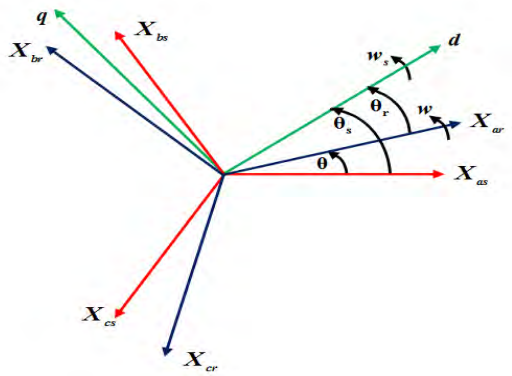

Fig.1.3-phase to 2-phase Axis transformation.

According to reference [3], the modelling of the motor involves assuming that a park reference frame is oriented with the magnetic field and rotates at a velocity of ωs. The matrix shown below directly define the park transformation:

$$\left[X_{dqo}\right]=\left[P\right]\left[X_{abc}\right] \quad (8)$$

Where:

$$\left[P\right]=\sqrt{\frac{2}{3}}\begin{bmatrix} cos(\psi) & cos\left(\psi-\frac{2\pi}{3}\right) & cos\left(\psi+\frac{2\pi}{3}\right) \\ -sin(\psi) & -sin\left(\psi-\frac{2\pi}{3}\right) & -sin\left(\psi+\frac{2\pi}{3}\right) \\ \frac{1}{\sqrt{2}} & \frac{1}{\sqrt{2}} & \frac{1}{\sqrt{2}} \end{bmatrix} \quad (9)$$

By applying the Park transformations in equations (1)-(4), then:

The stator windings:

$$\begin{aligned}\left[v_{s\_dq0}\right] &= \left[P_s\right]\left[R_s\right]\left[P_s\right]^{-1}\left[i_{s\_dq0}\right] \\ &+ \left[P_s\right]\frac{d}{dt}\left\{\left[P_s\right]^{-1}\left[\Phi_{s\_dq0}\right]\right\}\end{aligned} \tag{10}$$

$$\begin{aligned}\left[\Phi_{s\_dq0}\right] &= \left[P_s\right]\left[L_{ss}\right]\left[P_s\right]^{-1}\left[i_{s\_dq0}\right] \\ &+ \left[P_s\right]\left[L_{sr}\right]\left[P_s\right]^{-1}\left[i_{r\_dq0}\right]\end{aligned} \tag{11}$$

The rotor windings:

$$\begin{aligned}\left[v_{r\_dq0}\right] &= \left[P_r\right]\left[R_r\right]\left[P_r\right]^{-1}\left[i_{r\_dq0}\right] \\ &+ \left[P_r\right]\frac{d}{dt}\left\{\left[P_r\right]^{-1}\left[\Phi_{r\_dq0}\right]\right\}\end{aligned} \tag{12}$$

$$\begin{aligned}\left[\Phi_{r\_dq0}\right] &= \left[P_r\right]\left[L_{rs}\right]\left[P_r\right]^{-1}\left[i_{s\_dq0}\right] \\ &+ \left[P_r\right]\left[L_{rr}\right]\left[P_r\right]^{-1}\left[i_{r\_dq0}\right]\end{aligned} \tag{13}$$

Upon reduction of equations (10) and (12), the voltage expressions for a normalIM in the d-q-reference frame can be define by:

$$\begin{aligned}\begin{bmatrix} v_{\mathrm{sd}} \\ v_{\mathrm{sq}} \end{bmatrix} &= \begin{bmatrix} r_s & 0 \\ 0 & r_s \end{bmatrix}\begin{bmatrix} i_{\mathrm{sd}} \\ i_{\mathrm{sq}} \end{bmatrix} + P\begin{bmatrix} \Phi_{\mathrm{sd}} \\ \Phi_{\mathrm{sq}} \end{bmatrix} \\ &+ \begin{bmatrix} 0 & -\omega_s \\ \omega_s & 0 \end{bmatrix}\begin{bmatrix} \Phi_{\mathrm{sd}} \\ \Phi_{\mathrm{sq}} \end{bmatrix}\end{aligned} \tag{14}$$

$$\begin{aligned}\begin{bmatrix} 0 \\ 0 \end{bmatrix} &= \begin{bmatrix} r_r & 0 \\ 0 & r_r \end{bmatrix}\begin{bmatrix} i_{\mathrm{rd}} \\ i_{\mathrm{rq}} \end{bmatrix} + P\begin{bmatrix} \Phi_{\mathrm{rd}} \\ \Phi_{\mathrm{rq}} \end{bmatrix} + \\ &\begin{bmatrix} 0 & -(\omega_s - p\Omega) \\ (\omega_s - p\Omega) & 0 \end{bmatrix}\begin{bmatrix} \Phi_{\mathrm{rd}} \\ \Phi_{\mathrm{rq}} \end{bmatrix}\end{aligned} \tag{15}$$

: $P = \frac{\partial}{\partial t}$

Where:

$$\omega_s = \frac{\partial \theta_s}{\partial t}, \quad \omega_r = \frac{\partial \theta_r}{\partial t}, \quad \omega = \frac{\partial \theta}{\partial t} = p\Omega, \quad \omega_s = \omega_r + \omega$$

Ω: is the mechanical speed, ω: electrical speed.P: pole pairs

The equations of fluxes in (11) and (13) defined as:

$$\begin{bmatrix} \Phi_{\mathrm{sd}} \\ \Phi_{\mathrm{sq}} \end{bmatrix} = \begin{bmatrix} L_s & 0 \\ 0 & L_s \end{bmatrix} \begin{bmatrix} i_{\mathrm{sd}} \\ i_{\mathrm{sq}} \end{bmatrix} + \begin{bmatrix} M & 0 \\ 0 & M \end{bmatrix} \begin{bmatrix} i_{\mathrm{rd}} \\ i_{\mathrm{rq}} \end{bmatrix} \quad (16)$$

$$\begin{bmatrix} \Phi_{\mathrm{rd}} \\ \Phi_{\mathrm{rq}} \end{bmatrix} = \begin{bmatrix} L_r & 0 \\ 0 & L_r \end{bmatrix} \begin{bmatrix} i_{\mathrm{rd}} \\ i_{\mathrm{rq}} \end{bmatrix} + \begin{bmatrix} M & 0 \\ 0 & M \end{bmatrix} \begin{bmatrix} i_{\mathrm{sd}} \\ i_{\mathrm{sq}} \end{bmatrix} \quad (17)$$

Where in ref [4]:

$$L_s = l_{ls} + 1.5 l_{ms}, \quad L_r = l_{lr} + 1.5 l_{ms}, \quad M = 1.5 l_{ms}$$

The electromagnetic torque equations are defined by:

$$\begin{cases} \dfrac{\partial \Omega}{\partial t} = \dfrac{1}{J}\left(T_{em} - T_L - fv\Omega\right) \\ T_{em} = pM\left(i_{sq}\ i_{rd} - i_{sd}\ i_{rq}\right) \end{cases} \quad (18)$$

Where:

T_{em}, T_L, J and f_v are electromagnetic torque, load torque, inertia and viscous friction coefficient.

By setting ωs to zero in equations (14)-(15), the IM-model in the fixed reference frame can be realized.

2.2 Model Of 3-Phase IM under Open Phase Fault:

In the case of an open phase fault in a 3-phase induction motor, the dynamic performance of the machine changes significantly. Modeling of the IM under open phase fault conditions is essential to understand and predict the performance of the motor. The equivalent two-phase model, also known as the d-q model, is widely used to model induction motors under both normal and faulty conditions. When one phase of a 3-phase induction motor is lost due to an open circuit, the motor can still operate with an unbalanced winding and unbalanced excitation [14-18]. Nevertheless, the disconnected phase no longer interacts with the other phases through mutual coupling, leading to significant changes in the motor's behavior. The equivalent two-phase model for a 3-phase induction motor with an open phase fault includes two sets of equations: voltage equations and flux-current equations. The voltage equations describe the voltages induced in the stator windings due to the rotation of the rotor. The flux-current equations describe the link between the flux linkage and the rotor stator voltage and currents.Assuming a fault appears in phase "c" in the stator winding, resulting in an open circuit, as illustrated in Figure 2. [5].

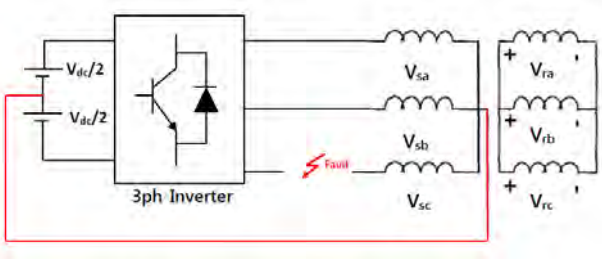

Fig.2.Open-phase fault conditionof 3-phase IM drive system.

Under unbalanced operating conditions, the flux and voltage equations forthe motor in the "abc" frame can be formulated as:

Stator:

$$\left[v_{s\_ab}\right]^{2\times 1}=\left[R_s\right]^{2\times 2}\ \left[i_{s\_ab}\right]^{2\times 1}+\frac{d}{dt}\left[\Psi_{s\_ab}\right]^{2\times 1} \quad (19)$$

$$\left[\Psi_{s\_ab}\right]^{2\times 1}=\left[L_{ss}\right]^{2\times 2}\ \left[i_{s\_ab}\right]^{2\times 1}+\left[L_{sr}\right]^{2\times 3}\ \left[i_{r\_abc}\right]^{3\times 1} \quad (20)$$

Rotor:

$$\left[v_{r\_abc}\right]^{3\times 1}=\left[R_r\right]^{3\times 3}\ \left[i_{r\_abc}\right]^{3\times 1}+\frac{d}{dt}\left[\Psi_{r\_abc}\right]^{3\times 1} \quad (21)$$

$$\left[\Psi_{r\_abc}\right]^{3\times 1}=\left[L_{rr}\right]^{3\times 3}\ \left[i_{r\_abc}\right]^{3\times 1}+\left[L_{rs}\right]^{3\times 2}\ \left[i_{s\_ab}\right]^{2\times 1} \quad (22)$$

In equations (19)-(22):

$$\left[R_s\right]_{2\times 2}=r_s\begin{bmatrix}1 & 0\\ 0 & 1\end{bmatrix}\quad \left[L_{ss}\right]_{2\times 2}=l_{ls}\begin{bmatrix}1 & 0\\ 0 & 1\end{bmatrix}+l_{ms}\begin{bmatrix}1 & -0.5\\ -0.5 & 1\end{bmatrix}$$

$$\left[L_{sr}\right]_{2\times 3}=l_{ms}\begin{bmatrix}\cos(\theta) & \cos\left(\theta+\frac{2\pi}{3}\right) & \cos\left(\theta-\frac{2\pi}{3}\right)\\ \cos\left(\theta-\frac{2\pi}{3}\right) & \cos(\theta) & \cos\left(\theta+\frac{2\pi}{3}\right)\end{bmatrix}$$

However, due to the asymmetrical structure of the stator windings in the studied IM, the commonly used (d-q) transformation defined in equation (9) will not be applicable. To examine the dynamic performance of the faulty 3-phase induction motor, its stator and rotor fluxes are represented in both the a-b-c and their equivalent d-q axes in stationary reference frame, as shown in Fig. 3 [6].

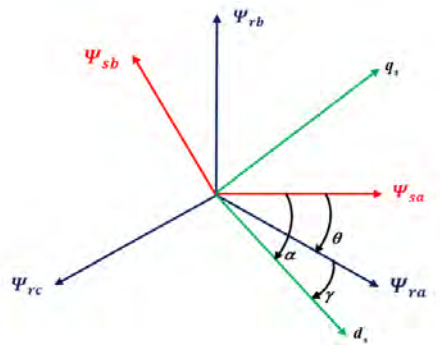

Fig.3. Axes of statorand rotor winding's flux at faultcondition.

The angles θ and α in Figure 3 correspond to the angle between the (as) and (ar) axes and the angle between the (as) and (ds) axes, respectively.

Hence:

$$\gamma = \alpha - \theta \quad (23)$$

Figure 3 presents the method for finding the normalized transformation of the rotor and stator modules, which is outlined in reference [6].

$$[P_s]^{Fault} = \frac{1}{\sqrt{2}} \begin{bmatrix} 1 & -1 \\ 1 & 1 \end{bmatrix} \quad (24)$$

$$[P_r] = \sqrt{\frac{2}{3}} \begin{bmatrix} \cos(\gamma) & \cos\left(\gamma + \frac{2\pi}{3}\right) & \cos\left(\gamma - \frac{2\pi}{3}\right) \\ \sin(\gamma) & \sin\left(\gamma + \frac{2\pi}{3}\right) & \sin\left(\gamma - \frac{2\pi}{3}\right) \end{bmatrix} \quad (25)$$

The new d-q model for the faulty motor in the stator reference frame is calculated by utilizing the transformation matrices $[Ps]^{Fault}$ and [Pr] to manipulate equations (19)-(22), as reported in reference [1]

Voltage equations:

$$\begin{bmatrix} v_{sd} \\ v_{sq} \\ 0 \\ 0 \end{bmatrix} = \begin{bmatrix} r_s + L_{sd} P & 0 & M_d P & 0 \\ 0 & r_s + L_{sq} P & 0 & M_q P \\ M_d P & p\Omega M_q & r_r + L_r P & p\Omega L_r \\ -p\Omega M_d & M_q P & -p\Omega L_r & r_r + L_r P \end{bmatrix} \begin{bmatrix} i_{sd} \\ i_{sq} \\ i_{rd} \\ i_{rq} \end{bmatrix} (26)$$

Flux equations:

$$\begin{bmatrix} \Psi_{sd} \\ \Psi_{sq} \\ \Psi_{rd} \\ \Psi_{rq} \end{bmatrix} = \begin{bmatrix} L_{sd} & 0 & M_d & 0 \\ 0 & L_{sq} & 0 & M_q \\ M_d & 0 & L_r & 0 \\ 0 & M_q & 0 & L_r \end{bmatrix} \begin{bmatrix} i_{sd} \\ i_{sq} \\ i_{rd} \\ i_{rq} \end{bmatrix} (27)$$

The following equation provides the new formula for the electromagnetic torque of a faulty IM:

$$T_{em} = p\left(M_q i_{sq}\ i_{rd} - M_d i_{sd}\ i_{rq}\right) (28)$$

Where in ref [1]:

$$L_{sd} = l_{ls} + 1.5 l_{ms}, L_{sq} = l_{ls} + 0.5 l_{ms}, M_d = 1.5 l_{ms}, M_q = 0.5\sqrt{3}\, l_{ms}$$

In a normal3-phase induction motor, the stator and rotor fluxes rotate in sync with each other and are aligned with the a-b-c coordinate system. However, under an open-phase fault condition, one of the stator phase windings is disconnected, causing a phase shift in the magnetic field. As a result, the stator flux rotates at a slower speed than the rotor flux and a phase shift occur between the two fluxes.This phase shift can be visualized on the d-q coordinate system, which is a rotating reference frame that follows the instantaneous position of the stator flux. In this coordinate system, the d-axis is aligned with the rotor flux while the q-axis is perpendicular to the d-axis.During normal operation, the stator flux is

aligned with the d-axis and there is no q-axis component. However, under an open-phase fault condition, the stator flux is no longer aligned with the d-axis and a q-axis component appears. This q-axis component causes an imbalance in the electromagnetic forces acting on the rotor, leading to increased vibrations and torque oscillations.In summary, under an open-phase fault condition, there is a phase shift between the stator and rotor fluxes, which can be visualized on the d-q coordinate system. The presence of a q-axis component in the stator flux can lead to increased vibrations and torque oscillations.

3. Simulation and Results

In this paper, simulations were conducted using the model presented in this paper to investigate the dynamic performance of a 3-phase IM under a phase fault or disconnected phase. The simulations were performed using M-File/MATLAB, where the IM was powered by a 3-phase network voltage. To solve theseequations of IM for both normal and faulty cases, the Runge-Kutta (RK4) method was employed.

In a normal3-phase induction motor, the stator and rotor fluxes rotate in sync with each other and are aligned with the a-b-c coordinate system. However, under phase fault condition, one of the stator phase windings is disconnected, causing a phase shift in the magnetic field. As a result, the stator flux rotates at a slower speed than the rotor flux and a phase shift occur between the two fluxes.

Table.1: The 3-phase IM under analysis is characterized by its electrical and mechanical parameters.

Rotor type	Parameters
Referenceframe	Stationary
Rated power	4 kW
Voltage	220/380 V
Frequency, *f*	50 Hz
Stator leakage inductance, l_{ls}	0.0068 H
Mutual inductance, *M*	0.15 H
Rotor leakage inductance, l_{lr}	0.0068 H
Stator resistance, *Rs*	1.2 Ω
Moment of inertia, *J*	0.05 kg.m^2
Rotor resistance, *Rr*	1.8 Ω
Number of pole pairs, *p*	2
Load torque, *TL*	25 N.m

These parameters are used in the simulation model to evaluate the dynamic performance of the induction motor under normal and faulty conditions.In order to investigate the dynamic behavior of the 3-phase induction motor under both normal and faulty conditions, a simulation is conducted using the proposed model and implemented in M-File/MATLAB. The simulation starts with the IM operating under normal conditions from t=0 s to t=2 s. At t=2 s, a fault is applied, where one of the phases is cut off, causing the motor to run under open phase fault conditions for $t \geq 2$ s. Furthermore, a load torque of 25 N.m is applied from t=1 s to t=1.5 s, to simulate a real-world scenario in fig4.

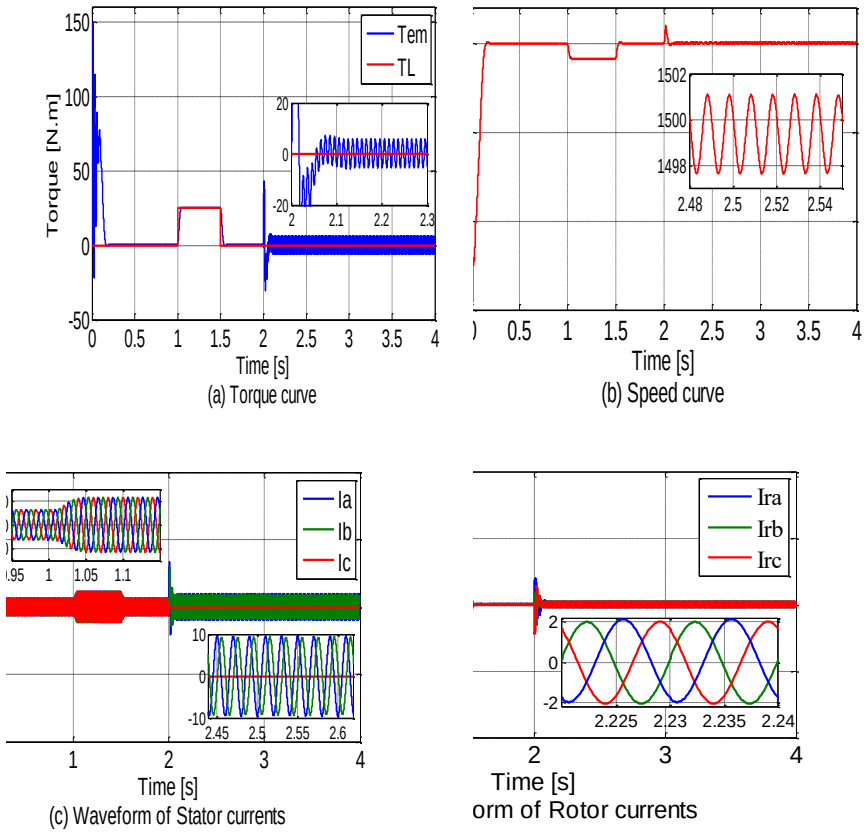

Fig.4. Simulation of IM under normal and fault scenario; (a) Torque; (b) Speed; (c) abc-stator currents; (d) abc-rotor currents.

As shown in the simulation results the phase fault caused an increase in the motor current and a decrease in the motor torque and speed. the fault effected significantly on the motor performance at and speed.

the rotor currents and torque oscillations were significantly increased compared to the normal condition. This is due to the unbalanced magnetic field caused by the missing stator phase, which causes additional torque pulsations and higher currents in the remaining phases. Additionally, the

rotor speed was found to be reduced under phase fault conditions, which is also attributed to the unbalanced magnetic field.

In general, the simulation results of the 3-phase IM under normal and faulty operations are presented in Fig. 4. Fig. 4(a) and Fig. 4(b) show the waveforms of torque and speed, respectively. It is observed that the fluctuations in torque and velocity show a rise upon the occurrence of the fault at t=2s. Fig. 4(c) shows the waveforms of abc-stator currents, where an increase in stator current is observed after the occurrence of the fault. Similarly, Fig. 4(d) shows the waveforms of abc-rotor currents, where an increase in rotor current is observed after the occurrence of the fault. These results confirm the impact of open phase fault on the performance of the 3-phase IM.

4. Conclusions and Perspectives

This paper presented a model of a 3-phase IM under open phase fault. The model was developed in the park reference frame and the effects of the fault were studied through simulations utilizingMatlab/M-file. The results showed that the oscillations of torque and velocity increasedat fault time, and there was also an increase in stator and rotor currents. Furthermore, the study demonstrated that the (d-q) transformation does not use to the asymmetrical stator windings configuration of the faulty IM. Therefore, a redefinition of the (d-q) transformation for the stator was necessary. The findings of this study are important for the maintenance and monitoring of induction motors, as faults can significantly affect their performance and operation. By understanding the effects of open phase faults, it is possible to take preventive measures and reduce the risk of damage or failure of the motor. Overall, the model developed in this study

provides a valuable tool for the analysis and prediction of the behaviour of 3-phase IM under open phase fault. In future works, exploring vector control of a 3-phase induction motor under open phase fault could provide further insight into the performance of induction motors during faults and aid in the development of fault-tolerant control strategies. Moreover, conducting investigations into the effect of different types of faults, such as inter-turn faults, could expand the applicability of the developed modelling method.

References

[1] S. V. Limaye and B. M. Jagadeesh, "Modeling and Simulation of an Open Phase Fault in a 3-Phase Induction Motor," International Journal of Innovative Research in Science, Engineering and Technology, vol. 4, no. 8, pp. 6909-6914, Aug. 2020.

[2] K. S. Sandhu and V. P. Singh, "Detection of Stator Winding Open Phase Faults in 3-Phase Induction Motors Using Mathematical Modelling and Simulation," International Journal of Advanced Research in Electrical, Electronics and Instrumentation Engineering, vol. 4, no. 8, pp. 7372-7383, Aug. 2021.

[3] M. Chitti Babu and P. Srinivasa Rao, "Simulation and Analysis of Open Phase Fault in 3 Phase Induction Motor Using MATLAB/Simulink," International Journal of Advanced Research in Electrical, Electronics and Instrumentation Engineering, vol. 2, no. 5, pp. 2025-2031, May 2022.

[4] M. Hanif, M. M. Nayeem, and M. O. Rahman, "Simulation of Open Phase Fault in 3 Phase Induction Motor Using MATLAB/Simulink," International Journal of Computer Applications, vol. 108, no. 16, pp. 28-32, Dec. 2022.

[5] S. P. Deepak, K. S. Mohan Kumar, and C. V. Jayadeva, "Detection and Classification of Open Circuit Faults in 3 Phase Induction Motors Using WPT and

ANFIS," International Journal of Computer Applications, vol. 47, no. 4, pp. 1-6, June 2021.

[6] V. B. Baru, A. K. Singh, and R. P. Yadav, "Detection of Open Phase Faults in 3-Phase Induction Motor Using MATLAB/Simulink," Journal of Electrical and Electronics Engineering, vol. 8, no. 2, pp. 17-22, June 2019.

[7] S. Kundu, S. Basu, and S. Sengupta, "Detection of open-circuit faults in stator windings of 3-phase induction motors using wavelet transform," IEEE Trans. on Energy Conversion, vol. 22, no. 1, pp. 113-122, Mar. 2007.

[8] M. Popescu, A. Bitoleanu, and D. Trifa, "Modeling and analysis of the 3-phase induction motor with phase unbalance," Electric Power Systems Research, vol. 75, no. 1, pp. 48-55, Jan. 2005.

[9] R. Prasad and A.K. Tandon, "A new fault diagnosis scheme for 3-phase induction motor using artificial neural network," Electric Power Components and Systems, vol. 37, no. 9, pp. 983-1000, Sep. 2009.

[10] Y. Abdel-Rady I. Mohamed and M.A. Abido, "Particle swarm optimization-based direct torque control of 3-phase induction motor with stator winding faults," IEEE Trans. on Energy Conversion, vol. 27, no. 4, pp. 997-1004, Dec. 2020.

[11] P. M. Ferreira, J. M. Azevedo, and H. M. Araújo, “Fault detection in a 3-phase induction motor using a combined approach of wavelet, neural network, and fuzzy logic,” IEEE Transactions on Industrial Electronics, vol. 55, no. 12, pp. 4396-4405, Dec. 2017.

[12] G. R. Dehkordi, B. Fahimi, and M. N. Cirstea, “Modeling and simulation of 3-phase induction motor with stator winding fault,” in Proc. IEEE Int. Symp. on Industrial Electronics, vol. 1, pp. 168-173, Jul. 2019.

[13] B. Fahimi and G. R. Dehkordi, “Modeling and simulation of a 3-phase induction motor with broken rotor bars,” IEEE Transactions on Energy Conversion,

vol. 20, no. 4, pp. 825-833, Dec. 2005.

[14] R. M. F. Mansoor and J. M. Guerrero, "Advanced mathematical model for a 3-phase induction motor with a broken rotor bar fault," IEEE Transactions on Energy Conversion, vol. 25, no. 2, pp. 545-552, Jun. 2010.

[15] S. Salahuddin, R. A. Ahmed, and M. A. Hannan, "Modeling and simulation of a 3-phase induction motor under inter-turn fault using MATLAB/Simulink," in Proc. IEEE Int. Conf. on Power, Control and Computer Vision, pp. 104-109, Dec. 2016.

[16] S. Kundu, S. Basu, and S. Sengupta, "Detection of open-circuit faults in stator windings of 3-phase induction motors using wavelet transform," IEEE Trans. on Energy Conversion, vol. 22, no. 1, pp. 113-122, Mar. 2018.

[17] S. A. Khan, A. Ahmed, and M. Iqbal, "Modeling and Simulation of Single-Phase Open Circuit Fault in Induction Motor," IEEE Power Engineering and Automation Conference, pp. 1-6, Nov. 2016.

[18] D. D. Handral, R. M. Metri, and R. K. Moger, "Modelling and Simulation of Open Circuit Fault in 3-Phase Induction Motor using MATLAB/Simulink," International Journal of Scientific Research in Science and Technology, vol. 2, no. 5, pp. 60-67, May 2016.

مجلة العلوم الشاملة

Journal of Total Science

البحوث المنشورة باللغات الأجنبية

Research Papers in Foreign Languages